



ELSEVIER

Contents lists available at ScienceDirect

# Quaternary Science Reviews

journal homepage: [www.elsevier.com/locate/quascirev](http://www.elsevier.com/locate/quascirev)

## The Prados del Cervunal morainic complex: Evidence of a MIS 2 glaciation in the Iberian Central System synchronous to the global LGM

Rosa M. Carrasco<sup>a,\*</sup>, Valentí Turu<sup>a,b</sup>, Rodrigo L. Soteres<sup>c,d</sup>, Javier Fernández-Lozano<sup>e</sup>, Theodoros Karampaglidis<sup>a</sup>, Ángel Rodés<sup>f,g</sup>, Xavier Ros<sup>b</sup>, Nuria Andrés<sup>h</sup>, José Luis Granja-Bruña<sup>i</sup>, Alfonso Muñoz-Martín<sup>i</sup>, José Antonio López-Sález<sup>j</sup>, Regis Braucher<sup>k</sup>, Javier Pedraza<sup>i</sup>, David Palacios<sup>h</sup>, ASTER Team<sup>k</sup>

<sup>a</sup> Departamento de Ingeniería Geológica y Minera, Universidad de Castilla-La Mancha, 45071, Toledo, Spain

<sup>b</sup> Fundació Marcel·lí· Chevalier, Andorra la Vella, Principat d' Andorra

<sup>c</sup> Centro de Investigación GAIA Antártica, Universidad de Magallanes, Punta Arenas, Chile

<sup>d</sup> Centro Internacional Cabo de Hornos (CHIC), Universidad de Magallanes, Puerto Williams, Chile

<sup>e</sup> Departamento de Tecnología Minera, Topografía y de Estructuras, Universidad de León, 24071, León, Spain

<sup>f</sup> Scottish Universities Environmental Research Centre, East Kilbride, G75 0QF, United Kingdom

<sup>g</sup> Currently at Departamento de Xeografía, Universidade de Santiago de Compostela, Spain

<sup>h</sup> High Mountain Physical Geography Research Group, Departamento de Geografía, Universidad Complutense de Madrid, 28040, Madrid, Spain

<sup>i</sup> Departamento de Geodinámica, Estratigrafía y Paleontología, Universidad Complutense de Madrid, 28040, Madrid, Spain

<sup>j</sup> Instituto de Historia, Consejo Superior de Investigaciones Científicas (CSIC), 28037, Madrid, Spain

<sup>k</sup> Aix-Marseille Université, CNRS, IRD, Coll. France, INRAE, UM 34, CEREGE, 13545, Aix-en-Provence, France

### ARTICLE INFO

#### Article history:

Received 27 February 2023

Received in revised form

30 May 2023

Accepted 2 June 2023

Available online 19 June 2023

Handling Editor: C. O'Cofaigh

#### Keywords:

Last Glacial Cycle

Global Last Glacial Maximum

Marine Isotope Stage 2

Last Deglaciation

Morphostratigraphy

Cosmic Ray Exposure dating

Iberian Central System

### ABSTRACT

The area of Prados del Cervunal (PC) is an intra-morainic topographic depression located at 1800 m asl in the divide or interfluvium between Garganta de Gredos and Garganta del Pinar valleys (Central Gredos; Iberian Central System, ICS). Both valleys, along with the adjacent Hoya Nevada, were occupied by glaciers during the Upper Pleistocene, leading to the development of the Prados del Cervunal moraine complexes studied in this work. Using cartographic methods and morphostratigraphic analysis, the three main glacial formations established in the Regional Chrono-Evolutionary Pattern for the ICS, Peripheral Deposits (PD), Principal Moraine (PM) and Internal Deposits (ID), have been identified and mapped in this area. The chronology of these formations has been implemented by Cosmic Ray Exposure (CRE) techniques using <sup>10</sup>Be (new data) and <sup>26</sup>Cl (previous data, recalculated in this work) in samples from morainic boulders. With these data, the following chrono-evolutionary sequence has been established: (stage 1) local-Maximum Ice Extent (MIE), dated in  $25.0 \pm 1.4$  ka and corresponding to the maximum age obtained in these paleoglaciators; (stage 2) period of oscillations around the MIE, corresponding to the development of the PD Formation between  $\sim 25$  ka and  $\sim 21$  ka; (stage 3) period of readvance and stabilisation, dated after  $\sim 21$  ka (average age obtained for the PD moraines attached to PM moraines) and previous to  $\sim 18$  (minimum age obtained for a main crest of the PM formation); and (stage 4) onset of deglaciation dated around to  $\sim 18$  ka (average of ages obtained for the first main crest of the ID formation). During the stages of maximum ice expansion, these three glaciers formed an Ice field whose tongues were interconnected on the PC flat by an ice transfluence system (stages 1 and 2, Plateau Glacier Period). In later stages, the ice masses were partitioned, giving rise to valley glaciers and large moraines forming morainic complexes like those of PC (stages 2, 3 and 4, Valley Glaciers Period). The local MIE and onset of deglaciation stages in this area show a good fit with the ages established to global level for the global Last Glacial Maximum (LGM) and the onset of the Last Glacial Termination (Termination I). They also show good correlation at local (with other areas of the ICS), peninsular (with other Iberian mountains) and continental (some areas of the Alps and mountains of Central Europe) level. Finally, this evolutionary sequence and its correlations allowed us to adjust and validate some units of the Regional

\* Corresponding author.

E-mail address: [rosa.carrasco@uclm.es](mailto:rosa.carrasco@uclm.es) (R.M. Carrasco).

Chrono-Evolutionary Pattern model and propose the Gredos-Pinar-Cabeza Nevada glacial system as benchmark for the glaciation of Marine Isotope Stage (MIS) 2 in the Iberian Peninsula.

© 2023 The Authors. Published by Elsevier Ltd. This is an open access article under the CC BY-NC-ND license (<http://creativecommons.org/licenses/by-nc-nd/4.0/>).

## 1. Introduction

The complex evolution of European glaciers at the end of the Last Glacial Cycle (LGC), with the culmination of the maximum glacial expansion, the onset of deglaciation, and the abrupt changes in climate leading up to the Holocene, is becoming increasingly well known for many of the European mountain massifs (Palacios et al., 2022). This is the case, for example, for the Alps (Ivy-Ochs, 2015; Ivy-Ochs et al., 2022, 2023) and the Tatra Mountains (Makos et al., 2018; Zasadni et al., 2022), and also for the Mediterranean mountains, such as those of the Anatolian Peninsula (Sarıkaya and Çiner, 2017; Akçar, 2022, 2023), the Balkans (Hughes et al., 2022a, 2023) the Apennines (Ribolini et al., 2022a, 2023) and the Iberian Peninsula (Turu et al., 2018; Oliva et al., 2019, 2022a, 2022b, 2023; Delmas et al., 2022, 2023). Most of controlling factors involved in glacier variations are already identified and rise challenging questions about the mechanisms responsible for natural climate variability in the past (Shakun et al., 2015). Outstanding drivers of these changes are: (1) the degree of insolation in the mid-latitudes of the Northern Hemisphere (Maslin, 2016); (2) the contribution of CO<sub>2</sub> in the atmosphere (Shakun et al., 2012); (3) sudden changes in air temperature (Rasmussen et al., 2014); (4) the isostatic rebound by the disappearing of glaciers (Gildor et al., 2014) and the relative sea level rising during and after the deglaciation (Lambeck et al., 2014); (5) changes in the sea ice extent (Bereiter et al., 2018) and variations in sea temperature (Sánchez-Goñi et al., 2008), partly due to meltwater discharges; (6) the evolution of the large ice sheets themselves, whose collapse open up large marine sectors as sources of moisture (Gildor et al., 2014); (7) and, finally, changes in the intensity of the Atlantic Meridional Overturning Circulation, that amplify the response of the driven mechanism (Starr et al., 2021). All these mechanisms might lead to modifications in the general atmospheric circulation (e.g., the cooling of the North Atlantic eventually weakens the Asian monsoon; Cheng et al., 2016) and causes the prevailing westerly winds and the Intertropical Convergence Zone, to migrate southwards (Toucanne et al., 2022) changing the proportion of dust in the atmosphere (Ellis and Palmer, 2016). The latter can be amplified by widespread volcanic activity and the emission of ash into the atmosphere (Turu et al., 2021). To discriminate between all these mechanisms and to establish the degree of involvement of each of them in recent environmental changes, the data provided by glacial variations dated using high-precision chronologies are essential.

### 1.1. The mediterranean region

In this context, the glacial evolution of the Mediterranean mountains acquires a particular relevance, as they are located on the southern edge of the temperate region of the northern hemisphere (Allard et al., 2021), especially if we consider that many of the climatic changes that occur during deglaciation are inverse in each hemisphere, a behaviour that is still poorly explained (Barker et al., 2009; Svensson et al., 2020). Precisely, the substantial progress in the knowledge of Mediterranean glacial evolution shows significant age offsets that do not allow linking the atmospheric circulation with the chronology of the early deglaciation (Turu, 2023).

The maximum extent of glaciers in the Mediterranean region, at least with current knowledge, seems to follow distinct patterns (Turu, 2023). Some are coeval with the LGM (according to Clark et al., 2009, 26.5 ka to 19 to 20 ka; or Hughes, 2022, 29–19 ka), such as several of the Iberian mountains (Oliva et al., 2019, 2022b), the Apennines (Ribolini et al., 2022a) and the Anatolian peninsula (Akçar, 2022). This maximum extension was synchronous with the last minimum sea level (Lambeck et al., 2014), the lowest proportion of CO<sub>2</sub> in the atmosphere (Shakun et al., 2012) and cold and arid climatic conditions in the Mediterranean basin (Fletcher and Sánchez-Goñi, 2008). However, the maximum ice extent took place during MIS 5d in the central Pyrenees (Delmas et al., 2022; Turu, 2023) and during MIS 3 in the Balkans (Hughes et al., 2022a), when the European ice sheets were much smaller than during the LGM (Batchelor et al., 2019). Paleoclimatic approaches reveal that the LGM period was much more unstable than previously thought and, similarly, the atmospheric circulation changed drastically (Toucanne et al., 2022). In fact, alternating periods when the atmospheric Polar Front and associated jet stream were displaced as far south as 37° N and periods when they were displaced further north reaching 41° N. Although it is not yet clear how these dynamics influenced the evolution of the Mediterranean glaciers, as we only know the effects over the western European mountain ranges (Turu, 2023).

### 1.2. The inner Iberia MIS 2 glaciation

The Iberian Central System (ICS) is located in the central part of Iberian Peninsula, affected by the climatic conditions of the Mediterranean basin to the east and the Atlantic to the west. It constitutes a larger E-W (450 km) climatic, environmental and geographic barrier (González-Sampérez et al., 2010; Abel-Schaad et al., 2014; Wolf et al., 2021; Antunes et al., 2021), strongly influenced by the North Atlantic Oscillation, that controls the snowfall distribution (Voelker et al., 2009; López-Moreno et al., 2011; Durán et al., 2013; Naughton et al., 2016; Beghin et al., 2016; Sánchez-López et al., 2016; Alonso-González et al., 2020). The ICS highest altitude is reached in the Sierra de Gredos, where significant glaciers were emplaced during Pleistocene glaciations. Previous works using CRE methods allowed the identification of three main stages of moraine formation, all of them occurring during the MIS 2 and or transition MIS 3–MIS 2 (Palacios et al., 2011, 2012a; Carrasco et al., 2013a, 2015, 2022a; Domínguez-Villar et al., 2013; Pedraza et al., 2013).

Regarding the paleoclimatic implications and completing the data provided by Penck (1894), Obermaier and Carandell (1915) calculated the snowline altitude for the glacial maximum (located on 1800–1900 m asl) and present periods (located on 3000–3100) that correlate well with data obtained in modern studies (Pedraza et al., 2013; Carrasco et al., 2022a). Recently, van der Knaap and van Leeuwen (1997), Carrasco et al. (2018), Turu et al. (2018), López-Sáez et al. (2020) and Hernández et al. (2023), used lake and peat cores to study the paleoclimatic evolution of the ICS Late- and Post-glacial periods (MIS 2–MIS 1).

The morainic complex of PC is located between the two most significant glaciated areas of Gredos mountains, the so-called Garganta de Gredos and Garganta del Pinar valleys. The complex

is enclosed between lateral moraines, where all the glacial phases are well preserved. In addition, geophysical surveys have been carried out that allow us to interpret the existing relationship among subsurface geometry, surficial morphology and glacial evolution. More specifically, the identification in the subsoil of PC of partially buried moraines and a preglacial topography that conditioned its layout (Granja-Bruña et al., 2021), are necessary to explain the contribution of non-climatic factors in the dynamics of glaciers and, in this specific case, in those of the western Mediterranean region during the LGM and the initial stage of Termination I.

### 1.3. Rationale

To know the glacial evolution reflected in the PC, it is necessary to establish the morphostratigraphic succession and chronology of these morainic complexes. To achieve this, the following work sequence has been implemented: (1) basing the CRE sampling strategy on a detailed mapping of these morainic complexes, integrating surface and subsurface data and determining the morphostratigraphic succession; (2) using  $^{10}\text{Be}$ -CRE dating on the samples from the main moraines of the PC; (3) updating the previous chronological data from adjacent areas where  $^{36}\text{Cl}$ -CRE was applied (Palacios et al., 2011, 2012a), to improve the accuracy of the chronology of the main stages of the last glaciation; (4) obtaining the evolutionary sequence of these glaciers from their local MIE to the onset of the Termination I and integrating it in the context of the Regional Chrono-Evolutionary Pattern of the ICS (Pedraza et al., 2011, 2013); (5) correlating the glacial phases across the ICS and other mountain ranges at regional and continental scale, showing a MIS 2 glaciation type within the western Europe.

## 2. Geographical and geological setting

### 2.1. Regional context

The Cervunal Meadows (Prados del Cervunal, PC) can be classified as a depressional seasonal meadow (Weixelman et al., 2011) originated by an intra-morainic topographic depression and located at 1800 m asl (average altitude) in the interfluvium of the Garganta de Gredos (Gredos Gorge) and Garganta del Pinar (Pinar Gorge) paleoglaciers (López-Sáez et al., 2023). Both valleys show a U-shape morphology upstream from their confluence with the river Tormes, located in the central sector of the Sierra de Gredos (ICS). This area also hosts the highest peak of the Gredos range, the so-called Pico Almanzor with 2591 m asl (Fig. 1). During the upper Pleistocene, these gorges were occupied by ice, forming two of the main valley glaciers of the ICS (see Oliva et al., 2019; Carrasco et al., 2022a). These paleoglaciers contributed to the development of a large ice field in the region and a notable interconnected middle morainic complex, including paleolakes dammed within inter-ridge depressions (Pedraza et al., 2011, 2013; Carrasco et al., 2020; Granja-Bruña et al., 2021) (Fig. 2).

The lithologies of the PC bedrock area are porphyritic or no porphyritic biotitic granitoids (i.e., monzogranites, granodiorites) and, locally, with scattered enclaves of metamorphic rocks (GEODE, 2004). The Upper Pleistocene and Holocene sedimentary cover is mainly represented by glacial, periglacial and slope deposits, with minor lacustrine and fluvial deposits (Pedraza and Fernández, 1981; Muñoz et al., 1995; Marcos, 2000; García-Sancho et al., 2001; Carrasco et al., 2020, 2022a). According to the analysis of fault populations mapped in the ICS and other geostructural indicators, tectonic control on the fluvial, periglacial, and glacial processes has been remarkable in this area during the Quaternary (Martínez de Pisón and Muñoz-Jiménez, 1972; Carrasco, 1997; Pedraza and Carrasco, 2006; de Vicente et al., 2018).

The Sierra de Gredos shows a Mediterranean mountain-type climate, strongly influenced by its continentality (Köppen-Geiger Climate Classification Dsb and Dsc; AEMET/IPMA, 2011; Durán et al., 2013). In the upper PC area, around 2200 m asl, the mean annual temperatures range from 15.0 to 2.5 °C, with a summer maximum of 27.5 °C and a winter minimum of -5.0 °C. The mean amount of days/year having temperatures below 0 °C is 100–120. Total annual rainfall oscillates between 1400 and 1800 mm with common snow falls between November and May. The valleys are located within an intermediate topographic-ecologic level (Ormediterranean; from 1700 to 1900 m asl) with residual forests of Scots pine (*Pinus sylvestris*), mountain scrubs (*Cytisus oromediterraneus*) and meadows (*Nardus stricta*), such as those confined in the PC area. At the bottom of the valleys, the precipitation decreases to 800 mm, and the duration of the snow cover does not exceed two-three months while the dry season (from July to September) is markedly longer in time (Moreno-Arriba, 2010; AEMET/IPMA, 2011).

### 2.2. Glacial geomorphology and chronology: previous work and approach in this study

Although the first scientific references to the glacial morphology of the Sierra de Gredos date from the end of the 19th century, systematic studies began in the 20th century (between 1917 and 1939; see Pedraza and Carrasco, 2006 and their references). These data and those obtained through subsequent and more precise works (Martínez de Pisón and Muñoz-Jiménez, 1972; Pedraza and Fernández, 1981; Acaso, 1983; Palacios et al., 2011, 2012a; Pedraza et al., 2013; Carrasco et al., 2020, 2022a), allow to summarize that: (1) during the stage of Maximum Ice Extent in the Sierra de Gredos massif, a system of coalescent ice field type glaciers was formed; (2) this system later evolved into valley glaciers located on the northern slope and, locally on both sides, slope glaciers; (3) the maximum elevation of a single glacial cirque when evolved into valley/slope glacier in this area was 2550 m asl, the glacier with the maximum distance was 10.5 km and the minimum height of a glacial front was 1210 m asl (Carrasco et al., 2011a, 2022a).

According to previous studies (see Rubio et al., 1992; Carrasco et al., 2011b, 2015), the glacial deposits are diamictites mostly composed of cobbles, pebbles, and boulders of granite and migmatite lithology within a scant matrix. The greatest volume of these deposits is located on the valley sides forming lateral moraines with well-defined crest-shaped ridges. The deposits at the bottom of the valley are discontinuous because of some bedrock exposures. We distinguish: (1) a vertical accretion sequence of tills (subglacial lodgement and melt-out tills) which form the flat topography of the valley and (2) surficial debris accumulations forming morainic ridges (arcuate or crescentic ridges across the valley) or erratic boulders corresponding to ablation processes. Recent studies have described a third sedimentary unit at the bottom of the valleys and depressions, named “basal complex formation” (Carrasco et al., 2020): “plain with hydromorphic soils and grassland development, which represent the result of a complex sedimentary filling in which sequences of tills, fluvio-glacial and lacustrine deposits may appear”.

The first numerical chronology of the glacial stages in the Sierra de Gredos was based on  $^{36}\text{Cl}$ -CRE (Palacios et al., 2007, 2011, 2012a) and  $^{10}\text{Be}$ -CRE (Domínguez-Villar et al., 2013). These chronological data have recently been reviewed, considering the most accurate production rate for the Iberian Peninsula (Oliva et al., 2019). The results indicated that Gredos and Pinar glaciers reached their outermost glacial limit at ~26 and ~24 ka, respectively, coeval with the global LGM (Mix et al., 2001; Clark et al., 2009; Hughes and Gibbard, 2015; Hughes, 2022). The data from samples of minor

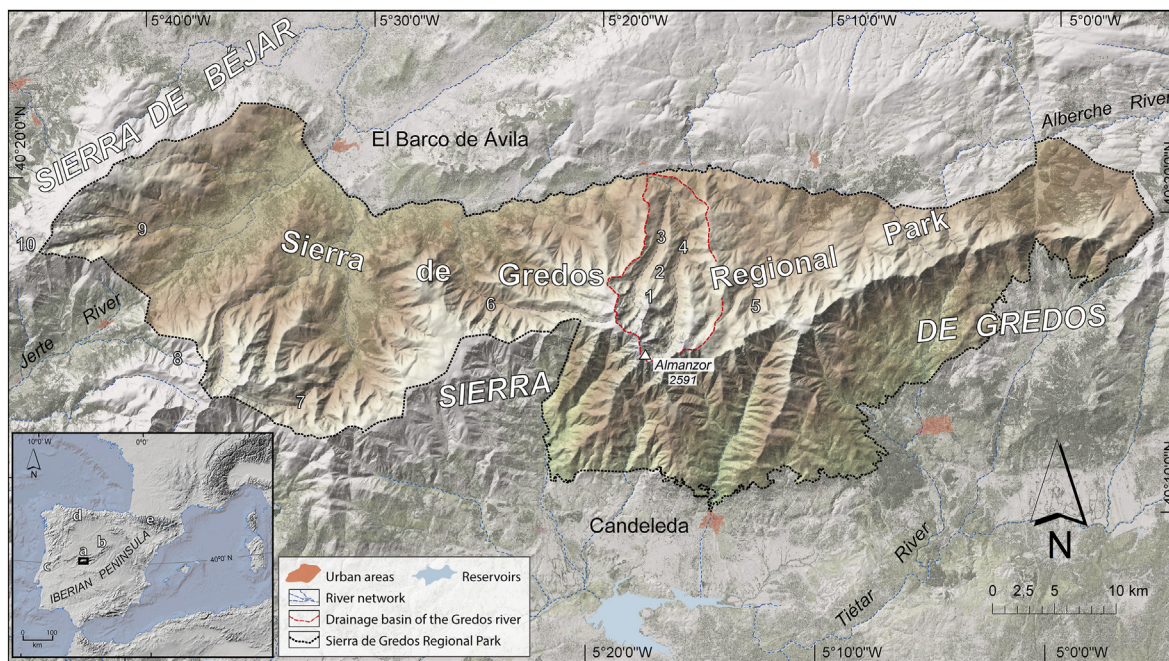


**Fig. 1.** Location of the study area in the context of the Sierra de Gredos. 1) Hoya Nevada valley, 2) Prados del Cervunal (PC), 3) Garganta del Pinar valley, 4) Garganta de Gredos valley, 5) Garganta de Las Pozas-Prado Puerto valleys, 6) Garganta de Bohoyo valley, 7) Garganta de los Caballeros valley, 8) Garganta de la Serrá valley, 9) Garganta del Duque-Trampal valleys, 10) Garganta de Cuerpo de Hombre valley-head, a) Sierra de Gredos mountains, b) Sierra de Guadarrama mountains, c) Serra da Estrela mountains, d) Cordillera Cantábrica-picos de Europa-Macizo de Trevinca mountains, e) Pirineos mountain.

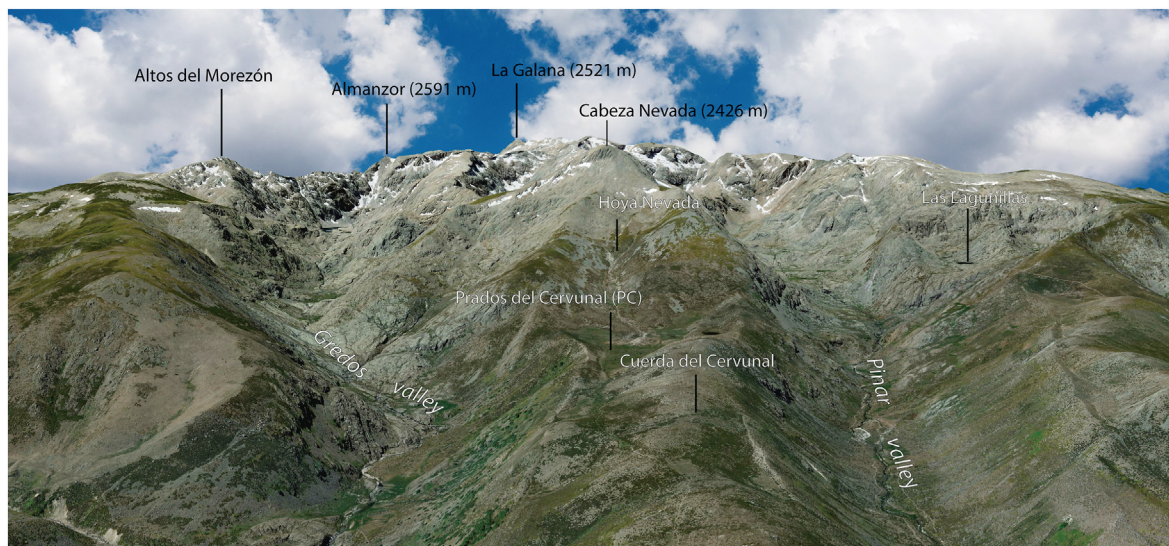


**Fig. 2.** 3D reconstruction based on the combination of 5 m-resolution LiDAR data and aerial orthophotography ([www.ign.es](http://www.ign.es)) of the Alto Gredos massif showing a panoramic view of the glacial cirques and valleys of the Gredos and Pinar gorges from the north (at the bottom of the image) to the south (at the top of the image).

moraine ridges close to the outermost limit and polished bedrock located upstream mark three post-maximum stages: (1) stabilisation before deglaciation at a minimum age of ~20 ka; (2) the beginning of the local deglaciation at a maximum age of ~17 ka; and finally (3), complete disappearing of the glacier at a minimum age of ~10 ka.

In the most recent works (Oliva et al., 2019; Carrasco et al., 2020, 2022a), these chronologies have been integrated into the context of the Regional Chrono-Evolutionary Pattern applied to ICS glaciers (Pedraza et al., 2011, 2013), which allowed establishing chronological and environmental correlations, both at local, regional, and global scales (Carrasco et al., 2015, 2018; Turu et al., 2018, 2021;

Oliva et al., 2019; López-Sáez et al., 2020). The main geomorphological unit used as reference to establish the morphostratigraphic succession in the ICS was the largest lateral or border moraines complexes called “principal moraine (PM)” formation (Pedraza et al., 2011, 2013). The PM was chosen as the best-preserved moraine morphology and the largest dimensions and from early research has been well identified in all paleoglaciers in the ICS. The PM is a closely nested morainic complex or polygenic formation elaborated in several evolutionary stages (Pedraza et al., 2011, 2013; Palacios et al., 2012b). The PM marks a readvance followed by a major stabilisation and, finally, the onset of the deglaciation (Carrasco et al., 2015). The deposits located in the outer position of

the glacial valley limited by PM formation (minor moraines and scattered boulders) are referred to as “peripheral deposits” (PD) formation. The deposits found in the inner of the glacial valley limited by PM formation (recessional moraines and scattered boulders) are referred as “internal deposits” (ID) formation. The geomorphological and genetic relations of these three formations present minor variations between the different paleoglaciers and its evolutionary significance has been shown to be generalizable to the entire Spanish-ICS (Pedraza et al., 2011, 2013; Carrasco et al., 2015, 2022a, 2022b; Turu et al., 2018; Oliva et al., 2019; López-Sáez et al., 2020). They represent: 1) the PD formation, corresponds to local MIE, subsequent oscillations, and a limited retreat; 2) the PM formation, corresponds to the mayor readvance and stabilisation and is the limit between de stages of glaciation and deglaciation; 3) the ID formation, corresponds to deglaciation stages.

### 3. Methodology

#### 3.1. Glacial Geomorphology

A revision of the Geomorphological Map of the Gredos and Pinar gorges by Carrasco et al. (2020) has been carried out, incorporating subsurface data obtained through geophysical and direct borehole investigations in PC (Granja-Bruña et al., 2021). These data have allowed specifying the limits of the maximum ice extent in each palaeoglacier, the different moraine complexes and the indicators of the relationships-interconnections between glaciers during their evolutionary stages. This cartographic revision has been carried out following the same procedures that are used for Carrasco et al. (2020), that is: using ArcGIS 10.4 software and 3D images from the IBERPIX viewer (IGN-IBERPIX); making the map through a previous photointerpretation (carried out with panchromatic stereo photos) and field checking (Smith et al., 2006; Chandler et al., 2018; Campos et al., 2018; Soteres et al., 2020; Leontaritis, 2021; Leontaritis et al., 2022); and using the classical structure of the legend for geomorphological maps (landform/deposit-process-age represented by symbols and colors patterns; Demek, 1972) and the most standardised symbols (FGDC, 2006). “This rigorous cartographic approach has provided: (1) a clear establishment of the morphostratigraphic succession; (2) improving the basis for the sampling strategy underpinning the chronological analyses, and (3) a robust understanding of the glacial evolutionary sequence and providing confidence in the correlations with other areas”.

#### 3.2. Surface exposure dating (CRE)

##### 3.2.1. Sampling

The sampling strategy aimed to obtain quantitative data on the age of boundary or transit indicators, with the outermost erratic boulders (Local Maximum Ice Extent indicators) and moraine crests (stage transit indicators) being the priority sampling targets.

In this study 22 new samples were collected for numerical exposure dating using  $^{10}\text{Be}$  in quartz from granitic boulders on moraines of the PC. These data are compared with further 10  $^{36}\text{Cl}$ -CRE ages previously obtained on boulders of these same moraine systems hosted in the Garganta de Gredos and Garganta del Pinar paleoglaciers (Palacios et al., 2011, 2012a) (Fig. 3A). To avoid till-shielded surfaces and to minimise the effect of potential boulder rotation, we sampled at least three large stable boulders on top of the crest from each moraine, with volumes larger than  $6\text{ m}^3$  (Dortch et al., 2013; Carrasco et al., 2015) (Fig. 3B1 to 3B4). We took the samples from flat surfaces and away from highly weathered areas, edges, joints, and cracks (Akçar et al., 2011; Stroeven et al., 2011). The samples were collected using a chisel and a hammer

from the upper surface of the boulders to a depth of up to 4–5 cm. A GPS recorded the sampling locations, and the dip/orientation of the sampling surface and the topographic shielding were measured with a clinometer and a compass.

All samples correspond to granites boulders (porphyritic monzogranite-granodiorite), from well-preserved surfaces, sometimes showing striations and polishings, and no signs of post-abandonment modifications, as all the moraines look well preserved. In some cases, the inner slopes of the lateral moraines show linear incisions due to paraglacial processes such as debris flow, particularly on the ridges of the ID formations (Carrasco et al., 2011b, 2020; Palacios et al., 2011, 2012a; Muñoz-Salinas et al., 2013). To avoid potential post-depositional displacements of the boulders, these incision points were ruled out for sampling. As the moraines are built by boulders and with minimal matrix (Rubio et al., 1992; Carrasco et al., 2011b), there are no fossilisation problems and given the altitude at which the samples were taken below 1800 m asl, the effects of snow cover are negligible.

##### 3.2.2. Data processing and exposure age calculation of $^{10}\text{Be}$ new samples and previous $^{36}\text{Cl}$ CRE ages

Exposure ages and uncertainties were calculated using the “CREP” (Cosmic Ray Exposure Program) online calculator (Martin et al., 2017; <http://crep.cirp.cnr.fr/#/>). In this work, we use the LSD (Lifton-Dunai-Sato) scaling scheme (Lifton et al., 2014), the ERA40 atmospheric model (Uppala et al., 2005) and the geomagnetic database based on the LSD Framework (Lifton et al., 2014), yielding a SLHL (Sea-Level-High Latitude)  $^{10}\text{Be}$  spallation production rate of  $3.99 \pm 0.22\text{ atoms g}^{-1}\text{ yr}^{-1}$ . To facilitate comparison with previous works, Table A1 and A2 (Appendix A) also shows the age results using the inputs and the time-dependent Lal/Stone scaling scheme (Lm; Balco et al., 2008). CREP online calculator produced ages 5 and 7% older with the LSD scaling scheme than when using Lm. The CREP model offers two types of uncertainties along with the ages: with and without the error arising from the production rate (external and internal uncertainties, respectively). The external uncertainties are indicated in brackets (Table 1).

The previous ages of  $^{36}\text{Cl}$  CRE from the Pinar and Gredos valleys are those initially established by Palacios et al. (2011, 2012a) and now recalculated according to Oliva et al. (2019) (Table 1). A comparative analysis of the CRE procedures using  $^{10}\text{Be}$  and  $^{36}\text{Cl}$ , Palacios et al. (2017) and Andrés et al. (2018) statistically indistinguishable and, hence entirely comparable, although the uncertainties of the  $^{36}\text{Cl}$  ages are much higher than the of  $^{10}\text{Be}$  ages.

### 4. Results. Chronology of the moraines sequence in Prados del Cervunal (PC) area

The morphostratigraphic succession of PC matches with that general established in the ICS (Pedraza et al., 2013; Carrasco et al., 2015, 2022a, 2022b; Oliva et al., 2019) (Fig. 3A, 4 and 5). The arrangement and characteristics of guiding formation, the PM, in Gredos and Pinar paleoglaciers are very similar. In many sections of both valleys, the PM is a large, very well-preserved moraine which is identified in the relief by the continuity and projection of its main crest, which separates the external domain (PD formations) from the internal domain (ID formations). However, in other sections of those same valleys, the deposits sit on the valley side and are formed only by boulder alignments (boulder trains), often scattered, making it more challenging to structure the different morphostratigraphic formations. This is the remarkable case of the left lateral moraines in the middle section of the Pinar paleoglacier (Fig. 6). The chronological data provided by the  $^{10}\text{Be}$ -CRE and  $^{36}\text{Cl}$ -CRE samples used in this work are shown in Table 1 and Fig. 4.

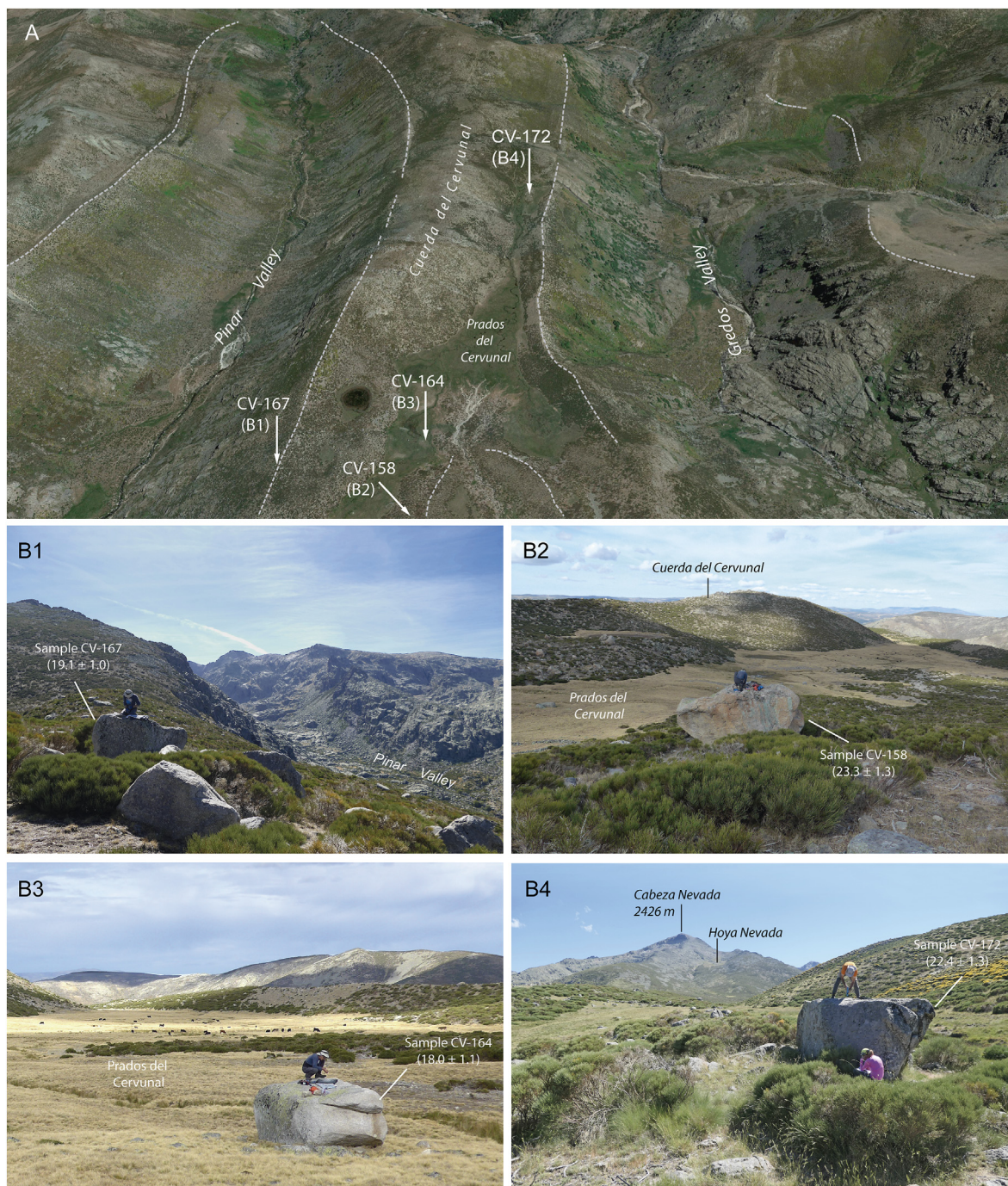


**Fig. 3.** A) 3D reconstruction based on the combination of 5 m LiDAR data and aerial orthophotography ([www.ign.es](http://www.ign.es)) showing from south to north the surrounding of the Gredos and Pinar valleys. The image shows the U-shaped valleys of Gredos and Pinar paleoglaciers, the Principal Moraine formation (PM; dashed line) and the position of four sampled boulders that appear in the below four images. B) Some examples of sampled boulder: (B1) Sample CV-167 was collected from a boulder on the right-lateral moraine of the Pinar paleoglacier (PM formation); (B2) Sample CV-158, collected from a boulder located on the minor moraines attached to the PM of the Hoya Nevada paleoglacier (PD formation); (B3) Sample CV-164, collected from a scattered erratic boulder of the PD formation located in Prados del Cervunal (PC); and (B4) Sample CV-172 was collected from a boulder on the left minor lateral moraine (PD formation) attached to the PM formation of the Gredos paleoglacier.

**4.1. The PC morainic complex: Gredos-Pinar-Hoya Nevada glacial system**

In this area, the PM formation is well preserved in these three paleoglaciers, which has facilitated the clear identification of the internal and external moraine complexes. All moraine ages correspond to samples of boulders located on their main crest. The

minimum boulder size sampled is 2.2 m<sup>3</sup>, with boulders up to 108 m<sup>3</sup> and an average of 22.3 m<sup>3</sup>.

The morphology of PD formation is represented here by a series of scattered erratic boulders (PDa) and minor moraines located on the eastern slope of the Cuerda del Cervunal (PDb). Minor moraines may be attached to/or partially covered (overlapping processes) by the PMs of the Gredos (PDC), Hoya Nevada (PDd) and Pinar (PDe)

**Table 1**

Geographic and cosmogenic isotopes analytical data sorted Garganta de Gredos, Garganta del Pinar and Hoya Nevada paleoglaciars. AMS standard NIST SRM 4325.1 $\sigma$  analytical or internal AMS uncertainties are shown.

Sample	Radionuclide	Latitude ( $^{\circ}$ N)	Longitude ( $^{\circ}$ E)	Elevation (masl)	ASTER ID	$^{10}\text{Be}$ (katoms/g)	$^{10}\text{Be}$ age (ka)
CV154	$^{10}\text{Be}$	40.2906	-5.2825	1796	CFIF	288.1 $\pm$ 9.2	20.3 $\pm$ 0.6 (1.1)
CV155	$^{10}\text{Be}$	40.2885	-5.2844	1843	CFIG	210.7 $\pm$ 7.3	14.7 $\pm$ 0.5 (0.9)
CV156	$^{10}\text{Be}$	40.2886	-5.2848	1838	CFIH	310.0 $\pm$ 10.0	21.1 $\pm$ 0.6 (1.2)
CV157	$^{10}\text{Be}$	40.2888	-5.2855	1839	CFII	349.0 $\pm$ 11.0	23.5 $\pm$ 0.7 (1.4)
CV158	$^{10}\text{Be}$	40.2893	-5.2893	1844	CFIJ	331.0 $\pm$ 12.0	22.3 $\pm$ 0.8 (1.3)
CV159	$^{10}\text{Be}$	40.2893	-5.2885	1831	CFIK	273.2 $\pm$ 8.8	18.9 $\pm$ 0.5 (1.1)
CV160	$^{10}\text{Be}$	40.2923	-5.2914	1858	CFIL	275.5 $\pm$ 9.0	18.7 $\pm$ 0.6 (1.1)
CV161	$^{10}\text{Be}$	40.2964	-5.2827	1778	CFIM	314.0 $\pm$ 10.0	22.2 $\pm$ 0.7 (1.3)
CV162	$^{10}\text{Be}$	40.2908	-5.2864	1805	CFIN	351.0 $\pm$ 13.0	24.2 $\pm$ 0.8 (1.5)
CV163	$^{10}\text{Be}$	40.293	-5.2873	1788	CFIO	312.0 $\pm$ 10.0	21.9 $\pm$ 0.6 (1.3)
CV164	$^{10}\text{Be}$	40.2914	-5.2882	1799	CFIP	253.7 $\pm$ 8.9	18.0 $\pm$ 0.6 (1.1)
CV165	$^{10}\text{Be}$	40.2900	-5.2892	1823	CFIQ	314.2 $\pm$ 9.7	21.6 $\pm$ 0.6 (1.2)
CV166	$^{10}\text{Be}$	40.2929	-5.2919	1835	CFIR	257.5 $\pm$ 7.3	17.9 $\pm$ 0.5 (1.0)
CV167	$^{10}\text{Be}$	40.2913	-5.2922	1864	CFIS	283.2 $\pm$ 7.5	19.1 $\pm$ 0.5 (1.0)
CV168	$^{10}\text{Be}$	40.2917	-5.2906	1831	CFIT	275.7 $\pm$ 8.9	19.1 $\pm$ 0.6 (1.1)
CV169	$^{10}\text{Be}$	40.2917	-5.2897	1822	CFIU	286.7 $\pm$ 8.2	19.9 $\pm$ 0.5 (1.1)
CV170	$^{10}\text{Be}$	40.3022	-5.2794	1778	CFIV	357.0 $\pm$ 10.0	25.0 $\pm$ 0.6 (1.4)
CV171	$^{10}\text{Be}$	40.3002	-5.2792	1762	CFIW	294.0 $\pm$ 10.0	21.1 $\pm$ 0.6 (1.2)
CV172	$^{10}\text{Be}$	40.2999	-5.2806	1767	CFIX	314.0 $\pm$ 10.0	22.4 $\pm$ 0.7 (1.3)
CV173	$^{10}\text{Be}$	40.2969	-5.2827	1776	CFIY	297.1 $\pm$ 8.2	21.1 $\pm$ 0.5 (1.1)
CV174	$^{10}\text{Be}$	40.2933	-5.2842	1786	CFIZ	335.2 $\pm$ 9.4	23.5 $\pm$ 0.6 (1.3)
CV175	$^{10}\text{Be}$	40.2935	-5.2834	1800	CFJA	310.0 $\pm$ 11.0	21.6 $\pm$ 0.7 (1.3)
						$^{36}\text{Cl}$ (katoms/g)	$^{36}\text{Cl}$ age (ka)
PINAR 07	$^{36}\text{Cl}$	40.3190	-5.2915	1595	–	530.8 $\pm$ 68.6	15.9 $\pm$ 2.6 (2.9)
PINAR 08	$^{36}\text{Cl}$	40.3157	-5.2929	1627	–	965.7 $\pm$ 318.8	21.4 $\pm$ 8.4 (8.8)
PINAR-09	$^{36}\text{Cl}$	40.3159	-5.2928	1620	–	744.6 $\pm$ 45.9	23.8 $\pm$ 2.2 (2.9)
PINAR-10	$^{36}\text{Cl}$	40.3163	-5.2922	1612	–	694.6 $\pm$ 117.9	18.7 $\pm$ 3.9 (4.2)
PINAR-11	$^{36}\text{Cl}$	40.3142	-5.2910	1626	–	621.3 $\pm$ 101.0	16.8 $\pm$ 3.3 (3.7)
PINAR-12	$^{36}\text{Cl}$	40.3147	-5.2910	1622	–	618.5 $\pm$ 77.3	14.9 $\pm$ 2.5 (2.9)
GREDOS-1	$^{36}\text{Cl}$	40.3002	-5.2609	1699	–	517.4 $\pm$ 20.7	24.5 $\pm$ 1.8 (2.5)
GREDOS-2	$^{36}\text{Cl}$	40.3009	-5.2621	1650	–	709.4 $\pm$ 31.8	24.1 $\pm$ 1.8 (2.3)
GREDOS-3	$^{36}\text{Cl}$	40.3023	-5.2647	1564	–	555.8 $\pm$ 29.1	22.8 $\pm$ 1.9 (2.3)
GREDOS-4	$^{36}\text{Cl}$	40.3036	-5.2668	1543	–	544.0 $\pm$ 16.1	22.8 $\pm$ 1.5 (2.1)

paleoglaciars deposits. The exposure ages, according to their location concerning the PM formations of the three paleoglaciars, are: in the PDA formation 21.9  $\pm$  1.3 ka and 18.0  $\pm$  1.1 ka; the PDb sample yielded an age of 25.0  $\pm$  1.4 ka; in PDC ages range between 23.5  $\pm$  1.3 ka and 14.7  $\pm$  0.9 ka; the PDD ages range between 24.2  $\pm$  1.5 ka and 21.1  $\pm$  1.2 ka; and finally, two PDe samples yielded the same age: 19.9  $\pm$  1.1 ka.

In the PM formation of each of the paleoglaciars the results obtained are: (1) in the left lateral PM of the Gredos valley (i.e., eastern boundary of PC), the samples yielded a range exposure ages of 21.6  $\pm$  1.3 ka and 21.1  $\pm$  1.2 ka; (2) in the right lateral PM of the Pinar valley (i.e., western limit of PC), the samples yielded a range exposure ages of 19.1  $\pm$  1.0 ka and 18.7  $\pm$  1.1 ka; and (3) in the PM of Hoya Nevada (i.e., southern limit of PC), sample yielded an age of 18.9  $\pm$  1.1 ka.

In the first recessional moraines attached to the inner slope of the PM and corresponding to the ID formation, the results obtained are: (1) in the left lateral slope of Gredos valley (i.e., eastern boundary of PC), sample yielded an age of 20.3  $\pm$  1.1 ka; and (2) in the right lateral slope of the Pinar valley (i.e., western limit of PC), the sample yielded an age of 17.9  $\pm$  1.0 ka.

#### 4.2. Left lateral moraines of the Garganta del Pinar valley: NW sector

$^{36}\text{Cl}$  data from Palacios et al. (2012a) have been revised and recalculated using CREP, as in Oliva et al. (2019). The samples were collected at the northwestern sector of this valley in a well-defined system of boulder alignments (boulder trains) covering several evolutionary stages. Based on the detailed mapping of Carrasco et al. (2020), the present work has determined the

morphostratigraphic succession of these alignments according to the sequence and terminology proposed in the Regional Chrono-Evolutionary Pattern for the ICS glaciers.

In the PD boulder alignments (PDe), three samples were reported by prior works, and the ages range between 23.8  $\pm$  2.9 ka and 15.9  $\pm$  2.9 ka. The PM boulder alignment sample yielded an age of 18.7  $\pm$  4.2 ka. Finally, the ID boulder alignments the sample yielded an age of 16.8  $\pm$  3.7 ka and 14.9  $\pm$  2.9 ka.

#### 4.3. Right lateral moraines of the Garganta de Gredos valley: SE sector

As in the previous area, available prior  $^{36}\text{Cl}$  dates (Palacios et al., 2011), were revised and recalculated with CREP. In this area, sampled boulders from several well-defined moraine arcs formed by glacier disfluency. The morphostratigraphic succession of these arcs has been determined, identifying first the PM and its main crest. With this reference, the PD and ID formations were later determined.

The outermost dispersed erratic boulders (PDA) sample yielded an age of 24.5  $\pm$  2.5 ka and the minor moraine attached to the PM (PDC) sample yielded an age of 24.1  $\pm$  2.3 ka. Finally, the samples collected in the ID Formation yielded ages of 22.8  $\pm$  2.3 ka and 22.8  $\pm$  2.1 ka.

## 5. Discussion

### 5.1. The geometry of the Gredos-Pinar-Hoya Nevada glacial system

In the PC area, only the two largest lateral moraines (PM or border moraines, Fig. 5) of the Gredos and Pinar glaciers that define

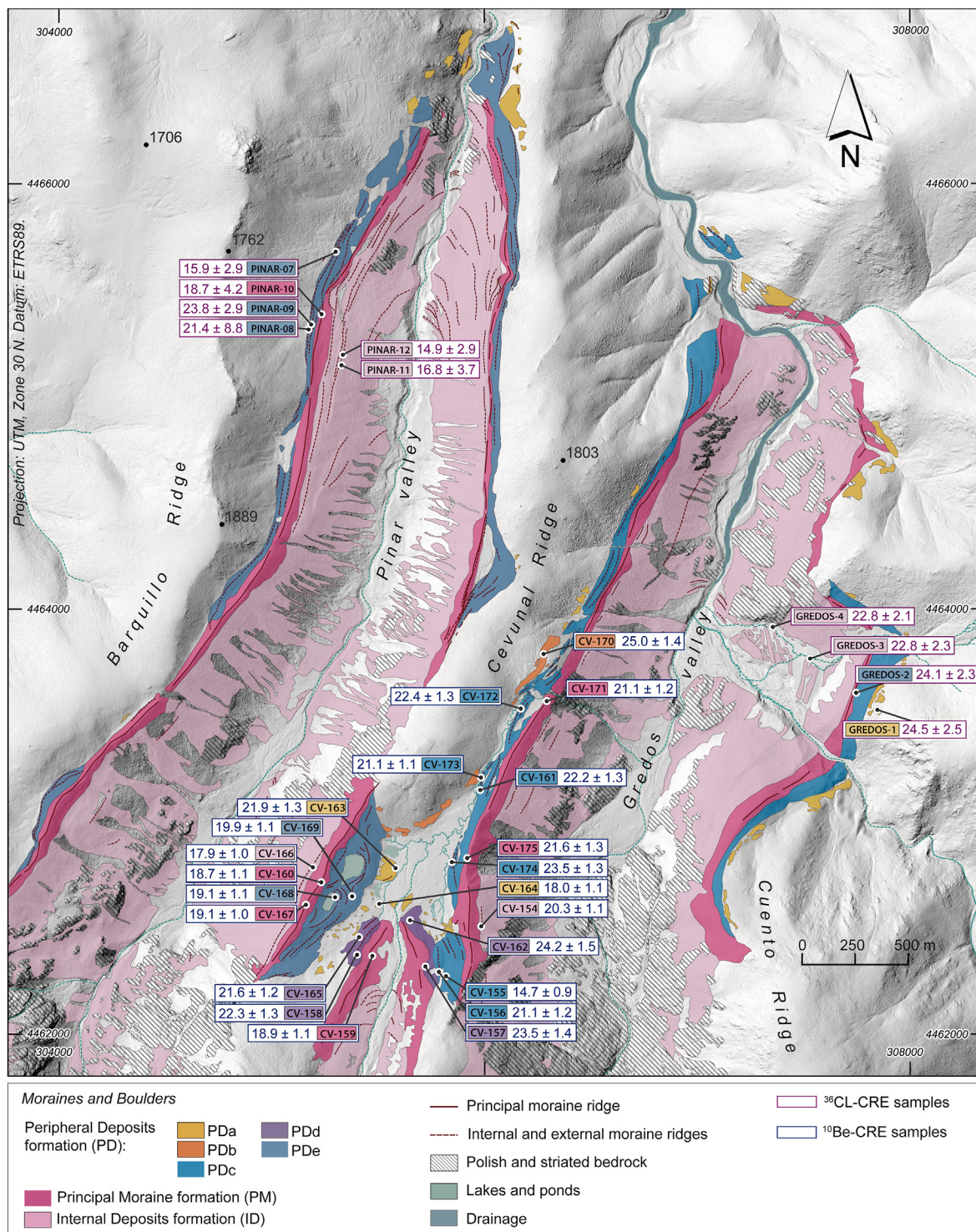


**Fig. 4.** Map of the moraine systems of the Gredos, Pinar, and Hoya Nevada paleoglaciers. The colors correspond to the morphostratigraphic formations identified in this area according to the sequence established in the Regional Chrono-Evolutionary Pattern for the ICS. In the boxes, are indicated the sample reference and the numerical values corresponding to the ages resulting from the CRE calculations.

the eastern and western limits of the depression were traditionally identified and considered the MIE of these glaciers (Obermaier and Carandell, 1916). Decades later, in the MAGNA Geological Map (Pedraza and Fernández, 1981), the small slope glacier of Hoya Nevada and their moraine complexes were mapped for the first time, although the scheme of the two large moraines (PM

moraines) as the outermost deposits and indicators of the MIE in this area was maintained (Fig. 5). More recent work (Palacios et al., 2011, 2012a; Pedraza et al., 2011, 2013; Carrasco et al., 2020, 2022a) identified new glacial deposits in PC located in the outer zones of the two large moraines which, accordingly, are no longer considered as the indicators of the MIE. In this context, the Gredos-Pinar-



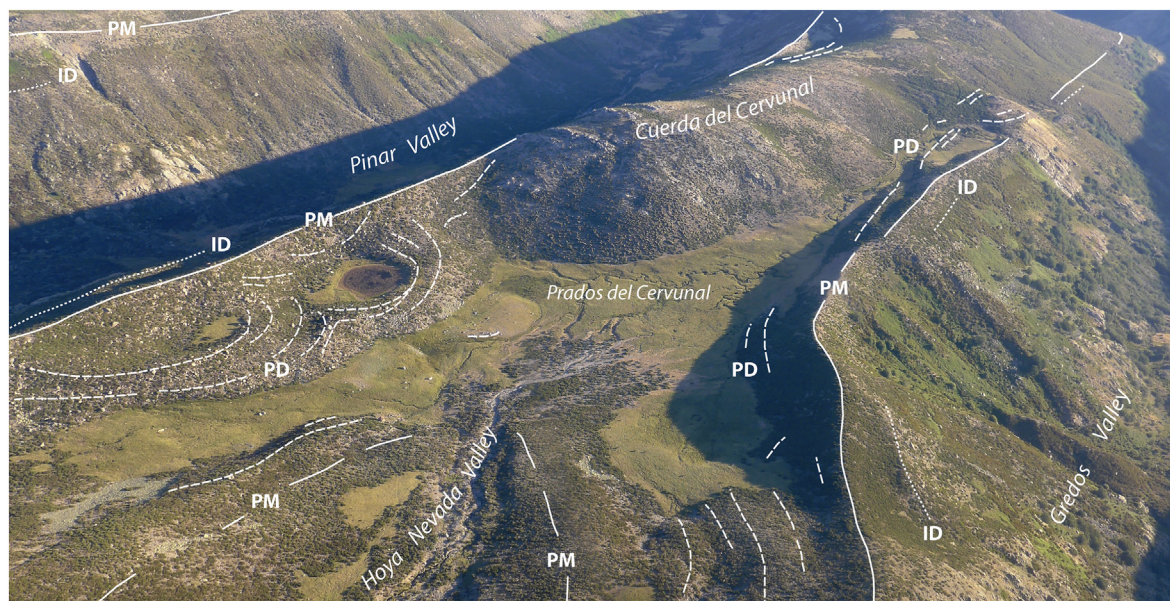


**Fig. 5.** Aerial view from south (at the bottom of the image) to the north (at the top of the image) of the Prados del Cervunal (PC) morainic complex. The dashed white lines represent morainic crests of the Peripheral Deposits formation (PD); the continuous white lines represent morainic crests of the Principal Moraine formation (PM); and the dotted white lines represent the outermost morainic crests of the Internal Deposits formation (ID).

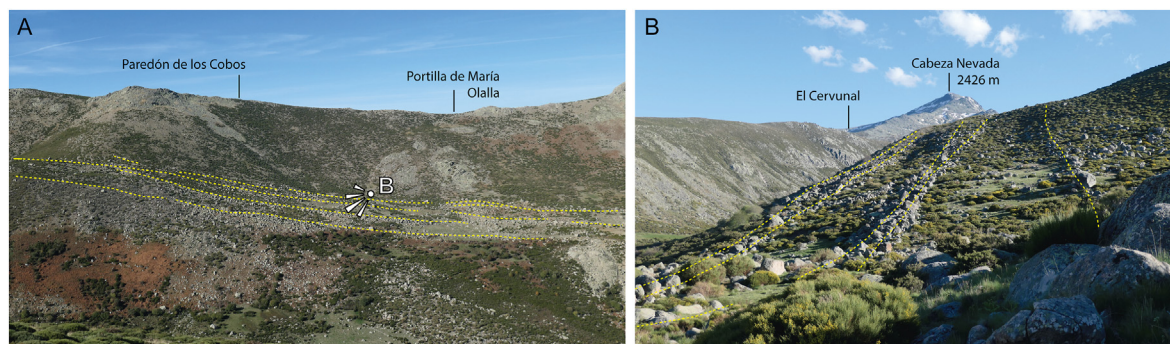


**Fig. 6.** Minor ridges of boulders (boulder trains) attached to the valley side forming the left lateral moraines in a sector of the Garganta del Pinar paleoglacier (A and B). This morphology, conditioned by the supplies of debris and the local topography, contrasts sharply with that of moraines well defined by large accumulations of materials forming mounds or larger ridges that stand out from the flat topography (see Fig. 5).

Hoya Nevada glacial system was catalogued with an integrated morphostratigraphic succession in the context of the Regional Chrono-Evolutionary Pattern, exhibiting well differentiated PD, PM, and ID moraine formations. However, all these works still consider that these glaciers were autonomous, with their tongues disconnected throughout their evolutionary sequence (Figs. 4 and 5).

According to the new indicators obtained in this study, the previous interpretation of the glacial morphology of PC must be modified. On the one hand, a system of scattered erratic boulders from the Garganta del Pinar paleoglacier indicates that there was an ice overbank system which penetrated into the PC domain connecting directly with the Hoya Nevada paleoglacier. On the other hand, studies using geophysical and borehole methods (Granja-Bruña et al., 2021), identified a buried moraine in total continuity with the surface expression of the limit between the Garganta de Gredos-Hoya Nevada glacial system (Carrasco et al., 2020). Moreover, the data provided by the chronology (Table 1, Fig. 4) supports the interpretation of Granja-Bruña et al. (2021) that this moraine was the central one separating the Pinar and Gredos paleoglaciers in their initial evolutionary stages. This implies the

existence of a large ice field connecting the three glaciers with remarkable topographic and structural control due to the preglacial valleys, divides, and hills. During the retreat of the glaciers after the MIE, the ice masses were progressively reduced in size, becoming compartmentalised and giving rise to autonomous glaciers causing the progressive nesting of the tongues in the valleys and, finally, restricted to the headwalls or cirques. The evolution of glacial features from a plateau-type to a cirque-type glacier, agree with previous descriptions of the ICS paleoglaciers (Carrasco, 1997; Carrasco et al., 2013a, 2015, 2016, 2022a; Pedraza et al., 2013). Similar sequences have also been described in other mountains in the Iberian Peninsula, such as the Trevinca Massif (Cowton et al., 2009) and the Cordillera Cantábrica and Picos de Europa ranges (Serrano et al., 2012, 2013a). In the PC area, this sequence can be described according to: (1) Plateau Glacier period with the three interconnected glaciers forming a large ice field in the Central Gredos area, from the inception and build-up of the glaciers to start of post-MIE major readvance (Fig. 7A, Table 2; from about 25 ka to 21 ka); (2) Valley Glaciers period, shows their maximum development during the stage of readvance post-MIE and, therefore, is

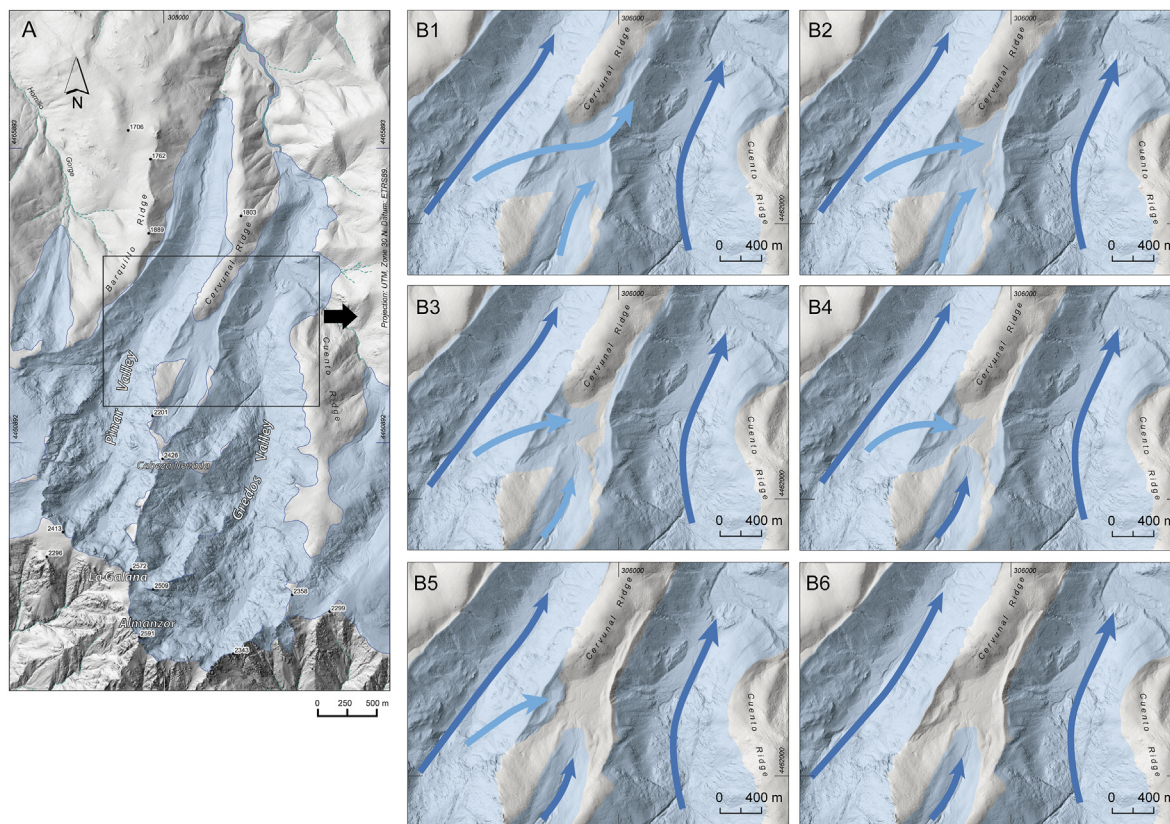


**Fig. 7.** Geomorphological interpretation of evolutionary sequence of the ice masses of the Gredos-Pinar-Hoya Nevada glacial system in Prados del Cervunal (PC) area, based on the mapping of the moraines during different evolutionary stages and according to the morphostratigraphic succession. For such purposes, we used data from the surface morphology, the geometry of the subsurface from geophysics and the chronology of the moraines from  $^{10}\text{Be}$ -CRE. The references to stages and geometry of the head of the glaciers (beyond the study area of the PC) were based on data from previous work (Pedraza et al., 2013; Carrasco et al., 2022a). A) General view of the Alto Gredos ice field during the local MIE stage. B) Evolutionary sequence of ice masses of this glacial system, from the MIE stage to onset of the deglaciation period (see Table 2). B1 to B3, Plateau Glacier period (from about 25 ka to 21 ka); (B1) local MIE stage, the total interconnection between the three glaciers at the head and ice transfluence from the Pinar valley to the Gredos valley, connecting the three glacial tongues; (B2 and B3) post-MIE minor retreat stage, beginning of the disconnection of the tongues between the three valleys giving rise to scattered erratic boulders and minor moraines of the PD formation. B4 to B6, Valley Glaciers period (from about 21 ka to 17 ka); (B4 and B5) ending of the post-MIE retreat stage with the total disconnection of ice on the valleys and, progressively, on the plateau; (B6) change of trend, readvance and stabilisation of the glaciers originating the moraines corresponding to PM formation already characteristic of well-defined individualized glacial valleys. The arrows indicate the ice-flow: dark blue, ice flow in each individualized valley; and light blue, transfluence of the ice.

coeval with the PM moraines which acts as true border moraines of the three independent valleys (Fig. 7B and Table 2; from about 21 ka to 17 ka); and (3) Cirque Glaciers Stage, no analysed in this paper, which are the residual glaciers that mark the final retreat of the ice (after about 17 ka).

## 5.2. Chrono-sequence and correlations

The  $^{36}\text{Cl}$ -CRE and  $^{10}\text{Be}$ -CRE dates show a remarkable agreement in all cases, which allows for their combined use as already highlighted in other works (Palacios et al., 2017; Andrés et al., 2018). From this chronological data and the provided by the morphostratigraphic succession, properly correlated locally, can be applied to the whole Sierra de Gredos, allowing a high-resolution sequence for the glaciation stages in these areas. Finally, regional, and general correlations are included using the most significant and up-to-date data (Table 2, Fig. 8).

### 5.2.1. The Local Maximum Ice Extent (MIE) of Prados del Cervunal morainic complex. Inception and build-up of the Gredos-Pinar-Hoya Nevada glacial system

Several prior papers have reported the LGC-MIEs of many ICS glaciers (e.g., Carrasco, 1997; Pedraza et al., 2011, 2013; Palacios et al., 2011, 2012a, 2012c; Domínguez-Villar et al., 2013; Carrasco

et al., 2015, 2016, 2022a, 2022b; Oliva et al., 2019) and even the glacial activity of a prior LGC glaciations (Vieira et al., 2021). These glacial chronologies have been obtained from samples of erratic boulders far from the axial zone of the valleys, and which are frequently associated with other boulders originated by slope processes, periglacial processes and even exhumation processes of the granitic alteration mantle. Due to these uncertainties, the mapping of the morphostratigraphic formations is a reference base, as it allows the reconstruction of the outline of some glacial morphologies that were poorly marked in the topography or that have been masked by other subsequent processes.

In the case of the PC, the local MIE is  $25.0 \pm 1.4$  ka and has been obtained in a well-catalogued boulder assigned to the PD formation of the glacial deposits of the left lateral margin of the Garganta de Gredos paleoglacier (Fig. 3A and 4). Regarding other ages obtained in this same PD formation, the PC local MIE is coeval with the maximum age recorded on the right slope of the Gredos paleoglacier ( $24.5 \pm 2.5$  ka; Palacios et al., 2011; Oliva et al., 2019) and, considering the margin of uncertainty in the dating, it is coeval with the maximum age recorded on the left slope of the Garganta del Pinar paleoglaciers as well ( $23.8 \pm 2.9$  ka; Palacios et al., 2012a; Oliva et al., 2019).

All these ages indicate that the two largest paleoglaciers of the Central Sierra de Gredos present a local MIE occurring within MIS 2

**Table 2**  
Chrono-evolutionary sequence and correlations of the Gredos- Pinar-Cabeza Nevada glacial system based on the chronological data available from  $^{10}\text{Be}$  and  $^{26}\text{Cl}$ -CRE and according to the Regional Chrono-evolutionary Pattern.

<b>MORPHO-STRATIGRAPHIC FORMATION</b>		Peripheral Deposits (PD): B (scattered boulders) and M (minor moraines)		Principal Moraine (PM)	Internal Deposits (ID)
<b>GLACIAL MORPHOLOGY</b>		PLATEAU GLACIER PERIOD		VALLEY GLACIER PERIOD	
<b>AGE (KY BP)</b> <b>LOCATION</b>	GP valley left	23.8 ± 2.9	21.4 ± 8.8 15.9 ± 2.9 <sup>a</sup>	18.7 ± 4.2	16.8 ± 3.7 14.9 ± 2.9
	GP valley right. PCMC	24.2 ± 1.5	23.5 ± 1.4	18.0 ± 1.1 19.1 ± 1.1 19.9 ± 1.1 21.9 ± 1.3 21.6 ± 1.2	17.9 ± 1.0 18.7 ± 1.1
	HN valley. PCMC			22.3 ± 1.3	18.9 ± 1.1
	GG valley left. PCMC	25.0 ± 1.4	23.5 ± 1.3 22.4 ± 1.3 22.2 ± 1.3 21.1 ± 1.2 21.1 ± 1.1 14.7 ± 09 <sup>b</sup>	21.1 ± 1.2 21.6 ± 1.3	20.3 ± 1.1
	GG valley right	24.5 ± 2.5	24.1 ± 2.3	–	22.8 ± 2.1 <sup>a</sup> 22.8 ± 2.3 <sup>a</sup>
<b>LOCAL PERIOD</b>		Maximum/ MIE	Post-MIE oscillations and limited retreat	Readvance and mayor stabilisation and started of deglaciation	The first stages of deglaciation
<b>REFERENCE AGE (Fig. 8; Appendix A3)</b>		25-23 ka	25-21 ka	21-19 ka	19-17 ka
<b>SOME CORRELATIONS USED IN THIS WORK</b>	Global event	LGM/glaciation (Mix et al., 2001; Clark et al., 2009; Hughes and Gibbard, 2015; Hughes, 2022)			Post-LGM/Deglaciation (Clark et al., 2009, 2012; Denton et al., 2010)
	Greenland chronology (Rasmussen et al., 2014)	GS-3	GS-3; GI-2.2; GI-2.1; GS-2.1c; GS-2.1b	GS-2.1b	GS-2.1b; GS-2.1a
	Local (ICS)	Sierra de Béjar (Carrasco et al., 2015, 2022a; Oliva et al., 2019); Sierra de Guadarrama (Palacios et al., 2012c; Carrasco et al., 2016, 2022b; Oliva et al., 2019); Eastern Sierra de Gredos (Alcalá-Reygosa et al., 2019)			
	Regional (Iberian Peninsula)	South-central Pyrenees (Pallás et al., 2006); Eastern Pyrenees (Delmas et al., 2008)		Sanabria Lake (Rodríguez-Rodríguez et al., 2014); Cordillera Cantábrica (Serrano et al., 2015); Cordillera Cantábrica (Frochoso et al., 2013); Pyrenees (most general age; Delmas, 2015; Delmas et al., 2023); Iberian Mountains (most general age; Oliva et al., 2019, 2023)	
Continental (Europe)	Tatra Mountains (Makos et al., 2014; Makos, 2015; Engel et al., 2015); Bohemia Forest (Mentlík et al., 2013); The Ticino-Toce glacier system (Alps, Kamleitner et al., 2022); The Southwestern Massif Central (France, Ancrenaz et al., 2022)			Eurasian Ice Sheet in SE England (Baykal et al., 2022)	
		The northern Alpine foreland: Rhine and Reuss glacier systems (Kamleitner et al., 2023)		Gerzensee Lake record (Switzerland)" (van Raden et al., 2013)	
				Alps (most general age; Ivy-Ochs, 2015; Ivy-Ochs et al., 2023); High Alps (Wirsig et al., 2016); Europa (most general age; Palacios and García Ruiz, 2015; Palacios et al., 2023)	

LGM: Global Last Glacial Maximum period; MIE: Local Glacial Maximum or Maximum Ice Extent; PCMC- Prados del Cervunal Morainic Complex; GP-Garganta del Pinar paleoglacier; GG-Garganta de Gredos paleoglacier; HN-Hoya Nevada paleoglacier.

<sup>a</sup> Samples that present discrepancy with the morphostratigraphic sequence defined in this work, due to possible distortions in the dating by "post-glacial toppling of the boulder or erosion of its surface" (see, Palacios et al., 2011, 2012a).

<sup>b</sup> Samples that present discrepancy with the morphostratigraphic sequence defined in this work, due to possible distortions in the dating by "post-glacial toppling of the boulder or erosion of its surface".

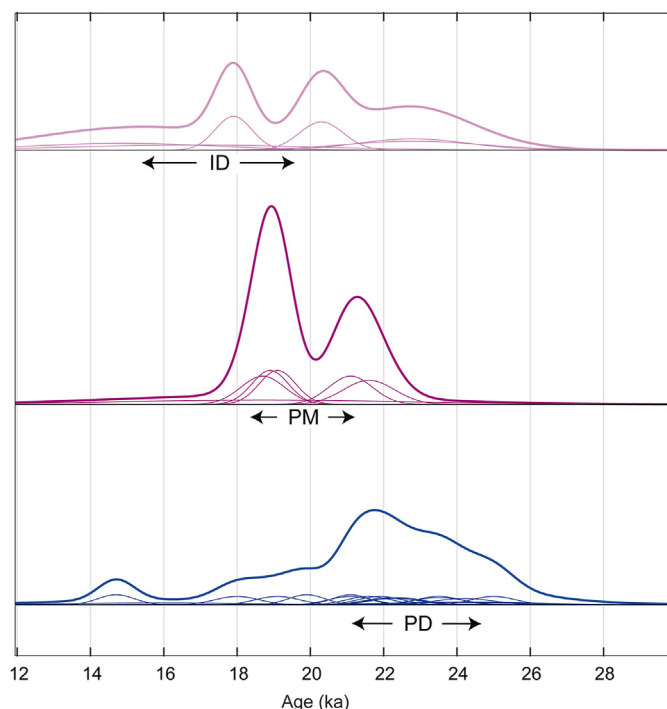


**Fig. 8.** Gaussian distributions corresponding to cosmogenic exposure ages and internal uncertainties grouped by the position of the samples in the moraine sequence (PD, PM, and ID). Sums of all distributions in the same group are depicted by a thick dark grey line. Below each distribution is shown the Gaussian age corresponding to each unit: PD:  $23.1 \pm 1.8$  (2.1) ka; PM:  $19.8 \pm 1.6$  (1.6) ka; ID:  $17.5 \pm 2.3$  (2.5) ka. See appendix A3 for details.

and coincident with the upper limit of the “Interval, period or time window” (Lambeck et al., 2010; Carrasco et al., 2015; Reber et al., 2022) considered as the global LGM (Mix et al., 2001; Clark et al., 2009; Hughes and Gibbard, 2015; Hughes, 2022). This agrees with data obtained in other ICS sectors, such as the Cuerpo de Hombre Valley (Sierra de Béjar, 40 km west of PC; Carrasco et al., 2015; Oliva et al., 2019) and the Los Pelados-El Nevero Massif (Sierra de Guadarrama, 154 km northeast of PC; Carrasco et al., 2016; 2022b). However, in other valleys of the ICS there are paleoglaciers with local MIEs occurring in the early MIS 2 or at the end of MIS 3, resulting ages between 31–27 ka. This is the case of the paleoglaciers Las Pozas-Prado Puerto and Garganta de Bohoyo (which were part of the Central Gredos ice field), Los Caballeros and La Serrá (28 km west-southwest of PC) and the Duque-Trampal system (35 km west of PC); all of them in the Sierra de Gredos (Domínguez-Villar et al., 2013; Oliva et al., 2019). This also occurs in the paleoglaciers of La Mujer Muerta and Peñalara (117 km and 130 km northeast of PC, respectively) in the Sierra de Guadarrama (Bullón, 2016; Palacios et al., 2012c; Oliva et al., 2019). Finally, the PC local MIE data obtained in this work are also asynchronous with those obtained in the westernmost sector of ICS, the Serra da Estrela (200 km west of PC), where the MIE-Local of the LGM has been assigned to MIS 3 and another one pre-LGM corresponding to MIS 6 (Vieira et al., 2001, 2021; Vieira and Woronko, 2022) (see, Fig. 1).

The existence of evolutionary mismatches or asynchronicities in glaciers fluctuations, is a fact analysed for years and supports the consideration of controlling factors to various levels of action and the refinement of dating procedures (Seret et al., 1990; Clapperton, 1993, 1995; Gillespie and Molnar, 1995; Giraudi and Frezzotti, 1997; Florineth and Schlüchter, 2000). It is well documented that the main evolutionary stages corresponding to the LGM (i.e., local MIEs, onset of deglaciation, stadial-interstadial sequences, etc.), do not

occur simultaneously in all regions (Ono et al., 2004; Thackray et al., 2008; Patton et al., 2013; Vasskog et al., 2015; Davies et al., 2018; Clark et al., 2022; Palacios et al., 2022, 2023), nor in all parts of the same region or mountain massif (García-Ruiz et al., 2003; Hughes et al., 2006a, 2006b; Ivy-Ochs et al., 2008; Larsen et al., 2009; Houmark-Nielsen, 2010; Böse et al., 2012; Domínguez-Villar et al., 2013; Dyke et al., 2014; Hughes and Woodward, 2017; Oliva et al., 2019, 2022a, 2022b; Allard, 2022; Ribolini et al., 2022b).

When these evolutionary asynchronicities occur between different sectors of large ice masses or a mountain range, regional climatic variables can be established as the leading cause of these evolutionary differences. This is the study case described in the Scandinavian, British and Irish Ice Sheets for the LGM and some stages of the Late Glacial (Böse et al., 2012). Also, in the Western Alps for the differences between the northern and southern MIEs (Gribenski et al., 2021; Ribolini et al., 2022b). In contrast, in the Pyrenees such mismatches were detected between closely spaced paleoglaciers (see García-Ruiz et al., 2003; Jalut et al., 2010; Calvet et al., 2011; Jiménez-Sánchez et al., 2013; Delmas, 2015; Delmas et al., 2022; García-Ruiz and Serrano, 2022) and was initially thought that to flaws in the dating/correlation procedures were the main causes of this asynchronicity (see Pallàs et al., 2006; Hughes and Woodward, 2008; García-Ruiz et al., 2010). However, after the application of multi-dating procedures and the refinement dating techniques, especially minimizing sampling bias and homogenisation of the CRE production rates applied, significant evolutionary gaps are still detected (Oliva et al., 2019, 2022a). In this regard, the data obtained in PC and, in general, in ICS, can be illustrative of the different approaches to this topic of asynchronicities.

The chronologies obtained in the ICS show remarkable asynchrony in the ages corresponding to the MIEs, being more homogeneous in the rest of the evolutionary stages (Oliva et al., 2019; Carrasco et al., 2022a, 2022b). Many of the MIE chronologies have been obtained by applying CRE techniques on isolated blocks of the PD formation, which implies some randomness in the identification/selection of samples. Therefore, when establishing causes of asynchronicities, this methodological factor cannot be ruled out. On the other hand, we must also work with the hypothesis according to which the chronological discrepancies may be due to differential behaviour of the controlling factors, e.g., the identification of a pre-LGM glaciation (Rissian, Alps; Saalian, northern Europe) only in Serra da Estrela, or the MIEs dated as MIS 3 and MIS 2 in the palaeoglaciers that were part of the same glacial system.

Regarding the first, and due to its differential climatic behaviour, a pre-LGM glaciation more extensive in the Serra da Estrela than in the rest of the ICS cannot be ruled out. This situation can be associated with the environmental variations in the ICS at the regional level, depending on the location of the mountain massifs (Turu, 2023) and their oceanic influence, maximum in Serra da Estrela (Vieira, 2008) and minimum in the Guadarrama and Somosierra mountain ranges (Carrasco et al., 2022b).

Related to the second, the temporal discrepancies detected even in neighbouring valleys, without ruling out potential dating flaws, the climate could partly explain the asynchronies in the ICS and other factors must be sought to explain these processes. Topography (pre-glacial morphology) and aspect can lead to differential mass balance by snow and ice avalanches, ice transfluences and snowdrifts. In several mountains areas, these processes and those due to topographic disconnections, have been described as responsible of differential evolution of glaciers, with notable contrasts in the development and flow of ice depending on their specific location within the same massif (Evans, 1977; Pratt-Sitaula et al., 2011; Yalcin, 2019; Pedraza et al., 2019; Boston and Lukas, 2019; Davies et al., 2022; Kaushik et al., 2022; Khandsuren et al.,

2022) which have proved very efficient in differential glaciers development (Mitchell, 1996; Purves et al., 1999; Coleman et al., 2009; Mîndrescu et al., 2010; Radbourne, 2015; Monegato et al., 2022). Regarding the latter, topography and aspect are the most likely controlling factors to explain the asynchronicities in the Bohoyo, Las Pozas-Prado Puerto and Gredos-Pinar-Hoya Nevada glaciers systems. During the inception and build-up of the local MIE, ice accumulation in these glaciers occurred on a connected system forming an ice field that had the cirques of the Gredos and Pinar paleoglaciers as its axial zone (Pedraza et al., 2013; Carrasco et al., 2020, 2022a). However, the resulting ages for the MIEs of these three glaciers show some dispersion, although they are concentrated in two groups, Bohoyo and Las Pozas-Prado Puerto corresponding to MIS 3–MIS 2 transition (see Carrasco et al., 2022a) and the Gredos-Pinar-Hoya Nevada, analysed here, to MIS 2.

### 5.2.2. The pre-MIS 2 MIEs in the ICS

The markers of the MIEs–LGC and of glaciations prior to the last one (pre-LGC), are boulders that rarely appear associated with well-defined glacial landforms, so there is a certain random component in the sampling, and we cannot be sure that we have sampled the oldest erratic boulders. However, the homogeneity of the chronological dataset obtained in Central Gredos consolidates these glaciers as a reference for the MIS 2 glaciation in Iberia (Turu, 2023). The presence of a local MIE boulder dated at  $31.9 \pm 2.3$  ka (MIS 3) in the adjacent valley of the Garganta de Bohoyo (Domínguez-Villar et al., 2013; Oliva et al., 2019) can be explained, by local topographic and microclimatic factors. Probably the plateau where the Bohoyo glacier belongs, a topographic-like control caused significant mismatches in the closer valley glaciers (Pratt-Sitaula et al., 2011; Kaushik et al., 2022), producing polythermal valley glacier having cold-ice above the ELA (Turu, 2023). These same factors can be considered to explain the small-time lags observed between the Gredos and El Pinar palaeoglaciers in the MIEs. On the other hand, considering the uncertainty factor in the chronology and the localised ages in the MIS 3–MIS 2 transition, all data support the development of large valley glaciers during MIS 2.

The lack of indicators of pre-LGC in the study area, it must be interpreted with great caution. As recent studies show in Serra da Estrela (Vieira et al., 2021), it is not ruled out that in the PD formations of this and other areas of the ICS (Spanish sector), there are some scattered boulders that can provide ages corresponding to earlier stages than those obtained so far (MIS 2–MIS 3). In fact, the hypothesis on the absence of pre-LGC glacier activity in the ICS never had much consistency. This is due to the presence of characteristic indicators of cold climate processes (slope deposits and soils) detected in the Spanish Central Plateau and ICS tentatively assigned to the penultimate glaciation (Rissian, Alps; Saalian, northern Europe; MIS 6) and those corresponding to the environmental changes occurred in the way to the Last Interglacial (Eemian; MIS 5e) (Butzer and Fränze, 1959; Vaudour, 1979; González-Martín and Pellicer-Corellano, 1988; Blain et al., 2017; Gil-García et al., 2019). In this context and given that the ICS is not a tectonically active area, where significant changes in topography during the Middle and Upper Pleistocene can be hypothesised (de Vicente et al., 2018), the best-founded explanation considers climatic and morphological constraints as limiting factors for the development of pre-LGC glaciation. In contrast to the Portuguese sector of the ICS (Serra da Estrela), the Spanish sectors (Sierras de Béjar, Gredos, Guadarrama and Somosierra) has a continental environment with a clear West–East climatic gradient marked both in the ELAs (Oliva et al., 2019) and in the ecological characteristics (Rubiales et al., 2010; López-Sáez et al., 2015; García-Antón et al., 2021; Liu et al., 2023). For this reason, moisture-laden Atlantic weather fronts arrive very weakened to the Spanish ICS (lesser

content of humidity) and other factors such as altitude and terrain morphology contribute to the development of the snow cover and, therefore, of glaciers compensating for the lack of precipitation. The altitudinal factor was favourable in most of the sectors of the Spanish ICS, since their summits are 300–500 m higher than the maximum altitude of the Serra da Estrela (Torre, 1993 m asl). As for the terrain morphology factor, as explicitly pointed out in several works (Vidal-Box, 1948; Martínez de Pisón and Muñoz-Jiménez, 1972; Sanz-Donaire, 1979; Martínez de Pisón and Palacios, 1997; Pedraza and Carrasco, 2006; Pedraza et al., 2019; Carrasco et al., 2022a, 2022b), numerous geomorphological indicators allow us to establish that the presence of pre-glacial valleys and fluvial catchments determined the development of glaciers in the Spanish ICS. As the sedimentary sequences show, one of the most critical stages for the consolidation of the modern drainage network in the fluvial basins of the Iberian plateau (Meseta) happened during the last interglacial (Eemian; MIS 5e) (Santisteban and Schulte, 2007; Pérez-González et al., 2008; Silva et al., 2012, 2017).

Therefore, considering the pre-LGC glacial cycle(s) as less extensive than the LGC due to non-climatic factors, i.e., the absence of suitable morphologies that would allow continuous for stabilised snow accumulations and, in turn, foster the development of large ice masses, may a consistent working hypothesis. Although derived from a lower-order local or regional context, this hypothesis supports the global ideas expressed in some works that consider Quaternary glacial processes to have a discontinuous evolution, sometimes controlled by their own dynamics (Hughes et al., 2020; Spagnolo et al., 2022).

### 5.2.3. The stages of transition post-MIE–Major readvance

The stages of transition post-MIE–onset of the readvance and formation of the PM moraine is defined by the first glacial retreats in the context of the LGM (first stage of the LGM period in this area). These are a series of oscillations around the maximum, but with a limited overall balance of retreat, originating boulder fields and minor recessional moraines that form the PD formation, whose chronology ranges from 25–23 ka (MIEs obtained in the outermost deposits of the formation) to 19–17 ka (ages obtained on the main crest of the PM formation).

The PM-marked stages of readvance–stabilisation correspond to a second maximum in these glaciers, which is also integrated within the LGM period (second stage of the LGM period in this area) and which is prior to the stages of deglaciation. This evolutionary sequence agrees well with the data obtained in several areas of the European continent, the Scandinavian ice cap or Greenland, which mark a series of retreat–readvance pulses within the LGM (Lambeck et al., 2010; Rasmussen et al., 2014; Hughes, 2022; Hughes et al., 2016, 2022b; Sinnl et al., 2022). In the case of PC, these are low magnitude oscillations similar, for example, to those detected in other sectors of the ICS, the Pyrenees, the Alps or Bohemia and have been described as “minor oscillations that kept the glacier front for several thousand years (LGM period or window) very close to its MIE or, where appropriate, LGM position” (Mentlík et al., 2013; Carrasco et al., 2015, 2016; Ivy-Ochs, 2015; Palacios et al., 2015; Oliva et al., 2019; Reade et al., 2020; Kamleitner et al., 2022, 2023).

### 5.2.4. Major post-MIE readvance and onset of termination I. Construction of the principal moraine (PM)

One of the main evolutionary stages for the construction of glacial morphology in the ICS was the major post-MIE readvance and stabilisation, represented by the large lateral moraines of the PM Formation (Pedraza et al., 2011, 2013; Carrasco et al., 2022a, 2022b). These moraines stand out in the relief and delimit the former glacial valleys, which is why in prior studies were considered the indicator of the MIE (see Pedraza and Carrasco, 2006 and

their references) before the identification of more external deposits (Carrasco, 1997).

Since the introduction of the term “Principal Moraine” (PM; Pedraza et al., 2011; 2013), it has been used in different works without specifying in detail its characteristics and evolutionary meaning (see Carrasco et al., 2022a, 2022b). Now we can say that it is a complex and polygenic lateral moraine (Pedraza et al., 2013; Palacios et al., 2012b), of multiple stacking by overlapping or attachment processes with previous and subsequent smaller moraines. In PC it appears very well defined and, therefore, we have been able to provide new data to validate the Regional Chrono-Evolutionary Pattern model (Figs. 5 and 9). Accordingly, when analysing the large lateral moraines of the ICS paleoglaciers that are generically referred to as PM, two different units must be considered: (1) the topographic physiognomy, which stands out in the terrain as an elongated mound (ridge) of non-unitary morphology, presenting several projections or slope breaks accounting for secondary ridges (Figs. 4 and 5); (2) the morphostratigraphic formation corresponding to the deposit of an entire evolutionary cycle indicated by the continuous accumulation of debris and is the one to be considered as PM in the strict sense (Pedraza et al., 2013; Carrasco et al., 2015). This second one, the PM (s.s.), has a clear main crest that represents the culmination of an evolutionary stage and marks the direction of the ancient glacier on the terrain.

In most paleoglaciers, the PM overlaps and fossilises part of the previous PD formation which, in general, corresponds to the MIE evolutionary stage defined by minor moraines and erratic boulders. On the other hand, some deposits accounting for several recessional moraines of the later ID formation are attached to its inner flank marking the initial stages of deglaciation. This sequence, documented for the ICS in general (Pedraza et al., 2011, 2013) and validated in several subsequent works (Carrasco et al., 2015, 2016, 2022a, 2022b; Oliva et al., 2019), is clearly marked in the PC and is a model to analyse the overlapping processes performed by the PM on the PD in the ICS paleoglaciers (Figs. 5 and 9).

Sometimes, the PM is a formation attached to the slope in which

it only stands out as a larger minor ridge than PD and ID formations (boulder trains; Fig. 6). Therefore, it is in the areas where the circum-glacial topography was favourable (saddles, bench, and shoulders on the slopes of glacier borders and, in general, flat morphologies), where the PM appears as a large alignment due to the sequential accumulation of deposits. This remarkable difference between the morphology of the deposits according to relief features are a clear example of the topographic control of moraines, a phenomenon widely described in many areas for its implications in making evolutionary and paleoclimatic inferences (Glasser et al., 2009; Pratt-Sitaula et al., 2011; Barr and Clark, 2012; Barr and Lovell, 2014; Yalcin, 2019; López-Moreno et al., 2020).

To explain the considerable development of the PM moraine and related to glacial dynamics, both intrinsic and extrinsic factors must be considered. The former includes the greater stabilisation of the glaciers, contributing to the over-accumulation of sediments in the ice-front and borders. As has been proposed in other areas, changes in the erosive capacity of the ice should also be considered (Marquette et al., 2004; Staiger et al., 2005; Ruszkiczay-Rüdiger et al., 2021). Extrinsic factors include overlap and fossilisation processes, but the most important was the increased debris supply due to increased wall instability on ice-free relief. This instability has been described in numerous papers, and which usually refer to the end of the LGM as one of the stages of enhanced gravitational processes (Cossart et al., 2008; McColl et al., 2010; Carrasco et al., 2013b; Pánek et al., 2016, 2023; Grämiger et al., 2017; Fernandes et al., 2020; Delaney and Anderson, 2022; Serra et al., 2022). In PC and, in general, in the ICS, this stage corresponds to the transition between the period of plateau glaciers to valley glaciers (Carrasco et al., 2013a, 2015, 2022a, 2022b). Last, the formation of the PM can be associated with three essential causes: (1) polygenic processes of overlap-fossilisation-attachment, (2) increased supply of debris and (3) duration of stabilisation after the readvance.

The above considerations on the characteristics of PM formation, while implicit in previous work, have not been formally described in any of them (see, Pedraza et al., 2013; Carrasco et al.,

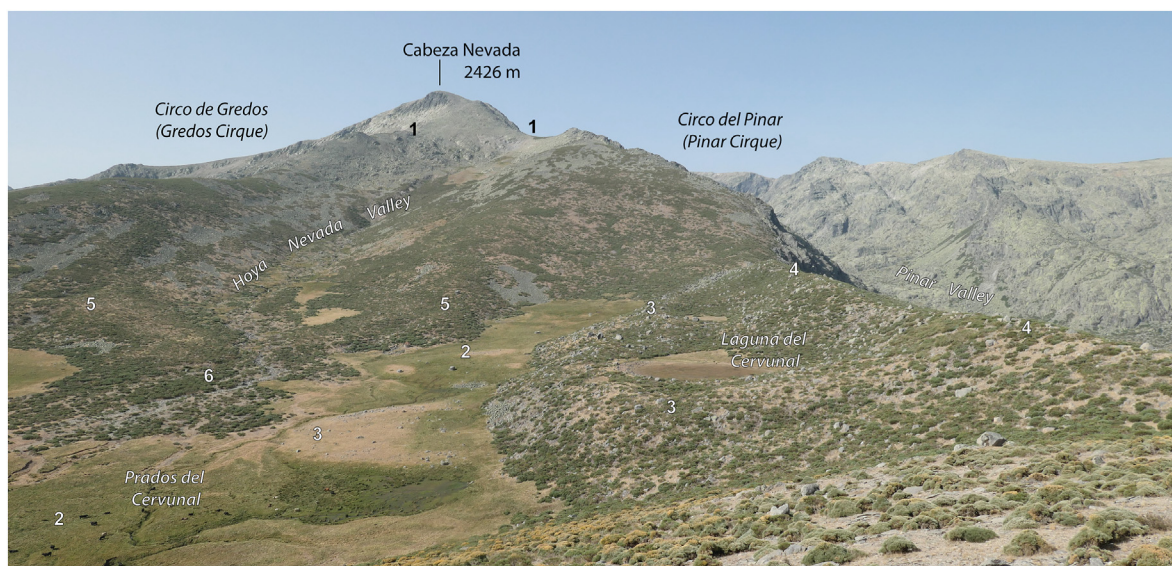


**Fig. 9.** Photograph of the southern sector of Prados del Cervunal (PC). The upper half of the image shows the slopes of the summit of Alto Gredos Massif. 1) Indicates the saddles of interconnection between the three paleoglaciers (Gredos-Pinar-Hoya Nevada) during the Plateau Glacier period (see Fig. 7). In the lower half of the image, most of the characteristic geomorphological elements of this area are visible: 2) PC plain with scattered erratic boulders of the PD formation corresponding to the first post-MIE retreat of the Gredos-Pinar-Hoya Nevada glacial system; 3) morainic lobes of the PD formation originated by the second post-MIE retreat of the Pinar glacier, already with its individualized valley but still penetrating into the PC zone; 4) left-lateral moraine of the PM formation corresponding to the Pinar glacier, which originated during the Post-MIE readvance (Valley Glaciers period, see Fig. 7) and cause the definitively obturation of the transfluence zone between the Pinar and Gredos valleys; 5) moraine system (PD and ID formations) of the Hoya Nevada paleoglacier already separated from that of Pinar and Gredos; 6) fluvio-paraglacial fan.

2015, 2022a, 2022b; Oliva et al., 2019). However, in the ICS this formation has been the fundamental guide to establish the evolutionary context of each paleoglacier and its correlations with prior studies. In this context of the PM and its evolutionary significance, the issue of the representativeness of each boulder as an indicator of the age of the landform (moraines in this case) has been raised in other areas, either because of post-sedimentary readjustments or because of its “ridge or slope” position (Putkonen and Swanson, 2003; Tomkins et al., 2021).

It is evident that not all sectors of a moraine have the same chronology, there are accumulations of debris, and the accretion-stacking process has a period of development. In the case of the PM, it is corroborated that each element of these moraines has a specific evolutionary significance (Figs. 5 and 9): (1) an overlapping outer ridge marks the limit of the post-MIE readvance and the beginning of the mayor stabilisation stage (in PC calculated around 21 ka); (2) the deposits on the outer slope of the PM are marking the stabilisation stage (in PC calculated around from 21 ka to 18 ka); (3) the main crest marks the end of this evolutionary sequence of readvancement-stabilisation and the beginning of the retreat or deglaciation stage (in PC calculated around 18 ka); (4) and, finally, the secondary ridges present on the inner slope of the MP mark the initial stages of the definitive retreat of the glacier (in PC calculated around 19–17 ka).

In short, in the characterisation of the PM as an indicator, it is necessary to differentiate: (1) the inception and build-up stage, which corresponds to the period of accumulation of debris due to the major readvance-stabilisation glacial events; (2) and its significance as a polygenic indicator, i.e. a sequence of stages indicating fossilised or overlapping deposits (previous stages of limited post-MIE retreat) and attached deposits (later stages of generalised retreat during deglaciation). Therefore, it is necessary to look for the sector of the main ridge or slope that best represents the change of trend (retreat to deglaciation - limit of the readvance and beginning of stabilisation). For this purpose, it is essential to determine the relationships between the main crest of the PM and the other morphologies: with the previous ones (PD Formations), to determine the end of the MIE-oscillations and the beginning of the readvance-stabilisation stage; and with the subsequent ones (ID Formations), to determine the end of previous stages and the onset of deglaciation period.

In order to date the PM unit in this area, ages obtained from the PD and ID units have been using as limiting maximum and minimum age distributions in the Bayesian approach explained in appendix A.3. Together with the data from PM samples, an average PM age of  $19.8 \pm 1.6$  ky was obtained (Fig. 8, Table 2).

### 5.2.5. The PM as principal indicator of MIS 2 events in the ICS

This post-MIE and pre-deglaciation stage of readvance-stabilisation has been described in numerous mountains of the Iberian Peninsula and is constrained with ages spanning from ~23 to 17 ka (i.e., MIS 2). The development of these processes has been variable, with notable differences even between very close areas. In some areas these readvances have presented a smaller extension reaching positions within the MIE geomorphological limits (Bordonau et al., 1993; Jiménez-Sánchez and Farias, 2002; García-Ruiz et al., 2010; Moreno et al., 2010; Delmas, 2015; Delmas et al., 2008, 2022; Frochoso et al., 2013; Jiménez-Sánchez et al., 2013; Gómez-Ortiz et al., 2012, 2015, 2022; Oliva et al., 2019). However, in other zones even in the same mountain chain, the glaciers reached positions very similar to the local MIEs and these readvances have been classified as a quasi-MIE or the second local MIE (Pallàs et al., 2006, 2010; Delmas et al., 2008, 2022; Serrano et al., 2012, 2013a, 2013b, 2015, 2022; Rodríguez-Rodríguez et al., 2014, 2015, 2016; Oliva et al., 2019; Ruiz-Fernández et al., 2016, 2022). A similar

evolution to the one described in the Iberian Peninsula has been found in other European mountain massifs, such as the Northern and Southern central Alps (Scapozza et al., 2014; Ivy-Ochs et al., 2022; Kamleitner et al., 2022, 2023), Maritime Alps and Apennines (Giraudi, 2015; Federici et al., 2017; Ribolini et al., 2022a, 2022b) or Tatra Mountains where they have also been considered as a second MIE known as LGM-II (Makos et al., 2014; Makos, 2015; Engel et al., 2015; Zasadni et al., 2022).

The causes of these minor glacial events during the LGM have been associated with the predominance of N-NW atmospheric situations that involved dry and cold weather during MIS 2 exacerbated during the Heinrich Events or Stadials (H) (Sarıkaya et al., 2008; Naughton et al., 2009, 2016, 2023; Serrano et al., 2012, 2013a; Domínguez-Villar et al., 2013; Ivy-Ochs, 2015; Ludwig et al., 2018; Rolland et al., 2020; Toucanne et al., 2015, 2022). However, this is a complex issue where one has to consider: (1) the evolution of climate and minor variations during the MIS 2 period (Hemming, 2004; Sarıkaya et al., 2008; Shakun and Carlson, 2010; Clark et al., 2012); (2) the existence within the LGM period and H events of minor stages or pulses in which ice stagnation, retreat or readvance processes alternate (Lambeck et al., 2010; Wýgal and Heidenreich, 2014; Toucanne et al., 2015; Sinnl et al., 2022); (3) the finding that in the Mediterranean region, H events involved glacial retreat stages due to climatic aridity (Allard et al., 2021); and (4) the finding that, at least in the European Alps region, during the LGM period there were changes in the dry Arctic-style precipitation regime and “the data provide compelling evidence that the LGM glacier advance in the Alps was fuelled by intensive snowfall late in the year, likely sourced from the Mediterranean Sea (Spötl et al., 2021)”.

Concerning to the readvance in this area of the Sierra de Gredos, according to the ages calculated for the PM and ranging between ~21–18 ka (Appendix A3, Table 2, Fig. 8) this process could be associated with the stage defined as pre-H1 (occurring between 20–19 ka; Naughton et al., 2023). Moreover, considering the mean value of the whole set of ages obtained on main crest of the PM formation (Table 2), the most probable age of the end of the readvance is between ~19–18 ka, i.e., within the H2–H1 transition stage (occurring between ~24–17 ka; Hemming, 2004).

Another important fact to consider in this stage of readvancement-stabilisation is the change in the morphology of the glaciers, whose tongues went on to have large volume but smaller extent than during the MIE stage. This process, also observed in the Sierra de Béjar (western sector of the Sierra de Gredos, ICS; Carrasco et al., 2013a; 2015), has been described in the Cantabrian Mountains and Picos de Europa and is associated with the change from more thermal glaciers during the MIE advance (pre-LGM) to colder ones in the LGM advance stages (Serrano et al., 2012, 2013a, 2015). This discrepancy between ice volume and ice extent it has also been raised on a regional and global (Peltier et al., 2021; Doughty et al., 2021) level as it has been detected that “world-wide many glacial systems of different sizes were more extensive during MIS 4 and MIS 3 than they were during MIS 2, stage during which they occurred the most recent maximum in global ice volume”. Doughty et al. (2021), in their model to explain these processes, suggest that climate is a determining factor in the configuration of ice masses, but non-climatic factors, including terrain topography, must also be considered.

In the case of the PC paleoglaciers and the ICS in general, there are no clear climatic indicators to support an overall increase in ice volume during the readvance stage compared to the MIE; both processes occur during MIS 2 and as previously described, the readvance is in the interval between the H2–H1 stadial. In this context, the processes of over-deepening in the MIE stage and the greater supply of debris during the post-MIE retreat (Carrasco et al.,

2013b), could have consolidated glaciers confined in the valleys limited by the lateral moraines of the PM formation and conditioned the geometry of the glacier masses, favouring the growth in volume of the tongues. At different spatiotemporal scale and basically focused on erosion processes, this type of “own-control” of glaciers over the configuration of their ice mass, has recently been proposed to explain the disagreements between the regional MIE of glaciers in Patagonia and the global minimum of temperatures and maximum volume of ice during the Quaternary Period (Kaplan et al., 2009).

According to the ages obtained in these deposits, the readvance and stabilisation process took place after ~21 ka (average of ages obtained for the ridges of the PD formation attached to outer slopes of the PM) and before ~ 18 ka (average of ages obtained for the ridges of the ID formation attached to inner slopes of the PM). Considering the new data obtained in the main ridge of the PM Formation, deglaciation in these valleys starts around 19–17 ka, similar to the ages previously obtained in these paleoglaciers and others in the ICS (Carrasco et al., 2022a, 2022b; Hernández et al., 2023) and most paleoglaciers of the Iberian Peninsula further north (Serrano et al., 2015; Rodríguez-Rodríguez et al., 2017, 2018; Oliva et al., 2019, 2023; Salvador-Franch et al., 2022; Ventura and Turu, 2022; García-Ruiz and Serrano, 2022; Ruiz-Fernández et al., 2022; Santos-González et al., 2022; Pérez-Alberti and Valcarcel, 2022). Moreover, it is coincident with that established in most northern hemisphere paleoglaciers, which place it around 20–19 ka, after the end of the LGM stage and prior to the H1 event (Clark et al., 2009, 2012, 2022; Denton et al., 2010; Hughes et al., 2013; Ivy-Ochs, 2015; Reade et al., 2020; Kamleitner et al., 2022, 2023). These similarities and the one pointed out for the MIE, already detected also in the western Sierra de Gredos (Cuerpo de Hombre paleoglacial, Carrasco et al., 2015), reinforce the consideration of the paleoglaciers analysed in PC as evolutionary referents of the MIS 2 in the central peninsular.

## 6. Conclusions

The data obtained by analysing the morphology and chronology of the PC moraines have allowed us to establish the evolutionary sequence of the ice masses of the Gredos-Hoya Nevada-El Pinar glacial system. In contrast to previous interpretations that considered the three glaciers to have independent tongues, this paper demonstrates that there was an interconnection between them in their upper section during the stages prior to the readvance stage (between approximately 25 and 20 ka). Associated with this interconnection, several transfluence processes have also been determined from the Pinar valley to those of Hoya Nevada and Gredos. This process has been interpreted as a conditioning factor of the topography (preglacial morphology) in the layout of the glaciers.

The sequence of the geomorphological formations of PC shows a good agreement with the ICS model, because the three main morphostratigraphic formations established in the Regional Chrono-Evolutionary Pattern (PD, PM, and ID) have been identified here. In addition, for the first time is presented a clear distinction between the PM as a unitary morphostratigraphic formation representing a specific evolutionary stage and the PM as a compound or polygenic physiographic unit due to overlapping and adjoining with the other formations (PD and ID). The origin of the PM is also associated with the increased supply of debris, due to the increase in para- and periglacial processes caused by the progressive retreat of the ice plateau at the head of the glaciers.

The chronological data obtained using  $^{10}\text{Be}$ -CRE show a good fit with those obtained previously using  $^{36}\text{Cl}$ -CRE. On the one hand, the results indicate that the glaciation in this area corresponds to

MIS 2, with the MIE (around 25 ka) and a major post-MIE readvance phase (around 21 to 19 ka), both within the LGM. These stages correlate well with those established in other sectors of the ICS and other mountains of the Iberian Peninsula and Central Europe. However, it differs from the more common sequence in the Mediterranean mountains. On the other hand, two of the leading evolutionary stages of these glaciers have been correlated with climatic events described in several European mountains (Pyrenees, Alps, ICS, Carpathians, Bohemia) and Greenland. This is the case of “intra-LGM” limited retreats and major-readvance post-MIE within the inter-HE stages. Therefore, it can be established that during the glaciation period (between MIE and the onset of the major readvance stage, about 25 and 21 ka respectively), the glaciers underwent only minor oscillations and their fronts remained close to their maximum extent or MIE. According to its chronological position, we consider that the recent model proposed for the Mediterranean region explains accurately the major readvance stage, locating the advance pulsations during the inter-HE stages, not within them.

All these chronological data obtained in PC support the hypothesis that the maximum development of the glaciations in the ICS corresponds to MIS 2. Many local MIEs are located at this stage or during the MIS 3-MIS 2 transit, especially the great post-MIE readvance that originated most of the current glacier morphology. This hypothesis is also supported by the characteristics of the indicators that mark glacial stages prior to the MIS 2, which, in general, are scattered erratic boulders or minor marginal moraines associated with the formations of the MIS 2 stages. However, so far not identified any pre-MIS 2 morphologically independent landform (morainic complexes, glaciated valleys, polish surfaces, etc.) in the ICS.

To establish the separation between the periods of glaciation and deglaciation and validate the data obtained through the chronologies, here we followed a morphostratigraphic criterion using geomorphological features as indicators of trend change, marking the beginning of evolutionary stage of deglaciation in the main crest of the PM. This is justified by the recessional nature of the post-PM moraines, as established in the Regional Chrono-Evolutionary Pattern. The average age obtained with this criterion is around 19–17 ka, which fits the proposed global age for the onset of deglaciation in the Northern Hemisphere.

Finally, the timing and configuration of the ice masses are partly associated with local topographic factors. The MIE and the onset of deglaciation occur slightly earlier in the Gredos paleoglacier, which could be due to the morphological configuration of its accumulation basin. The changes in the configuration of the ice masses detected during the stage of major readvance and stabilisation (PM formation) depict a glacier of a large volume but smaller extent than during the stages of MIE and oscillations post-MIE (PD formation). A similar process has been described in some mountains and is considered to have an essentially climatic basis. However, we also suggest the hypothesis of the morphological configuration as a factor associated with climate. Accordingly, in the stages prior to the major readvance (represented by the PD formation), the glaciers were more extensive but smaller in volume and with a predominance of erosive phases that were causing the progressive nesting of the tongues in the valleys. In the stages of the readvance and stabilisation (represented by the PM formation), the ice already appears channelled, and the greater supply of debris allows the formation of large lateral moraines (border moraines) that limit the lateral expansion of the tongue but would allow for larger ice accumulations. The retreat of these ice masses, correspond to the stages of deglaciation that formed the inner sequence of recessional moraines during the TI period.



## Declaration of competing interest

The authors declare that they have no known competing financial interests or personal relationships that could have appeared to influence the work reported in this paper.

Rosa M. Carrasco: coordination, mapping and sampling, data processing, wrote the paper with contributions from all coauthors, review and editing. Valentí Turu, Rodrigo L. Soteres, Javier Fernández-Lozano and Javier Pedraza: mapping and sampling, data processing, writing, editing and revision. Theodoros Karampaglidis and Ángel Rodés and Régis Braucher: TCN data processing, samples treatment, exposure age calculations, writing and revision; Régis Braucher supervised the Be ratio measurement at the AMS facility ASTER (CEREGE). Nuria Andrés and David Palacios: writing, editing and revision. Xavier Ros, José Luis Granja-Bruña, Alfonso Muñoz-Martín and José Antonio López-Sáez: writing and revision.

## Data availability

Data will be made available on request.

## 7. Acknowledgements

This work was supported by the Spanish Ministry of Science and Innovation (project PID2020-117685 GB-I00), Castilla-La Mancha University (UCLM, project 2023-GRIN-34112), ANID FONDECYT postdoctoral #3220537, ANID BASAL CHIC #FB210018 and ANID FONDECYT Regular #1220550. The ASTER AMS national facility (CEREGE, Aix-en-Provence) is supported by the INSU/CNRS, and IRD. The authors acknowledge the help and assistance received from the Sierra de Gredos Regional Park (Environmental Department of the Junta de Castilla y León, JCyL) and to the "Guardería" (Staff of surveillance and control) of the Gredos Regional Reserve for their remarkable help in the fieldworks. We also thank the Editor and reviewers, for their helpful comments and constructive suggestions that greatly improved this manuscript.

## Appendix A. Supplementary data

Supplementary data to this article can be found online at <https://doi.org/10.1016/j.quascirev.2023.108169>.

## References

- Abel-Schaad, D., Pulido, F., López-Sáez, J.A., Alba-Sánchez, F., Nieto-Lugilde, D., Franco-Múgica, F., Pérez-Díaz, S., Ruiz-Zapata, M.B., Gil-García, M.J., Dorado-Valiño, M., 2014. Persistence of tree relicts in the Spanish central system through the Holocene. *LAZAROA* 35, 107–131. [https://doi.org/10.5209/rev\\_LAZA.2014.v35.41932](https://doi.org/10.5209/rev_LAZA.2014.v35.41932).
- Acaso, E., 1983. Estudio del Cuaternario en el Macizo Central de Gredos. Tesis Doctoral. Facultad de Ciencias, Universidad de Alcalá (UAH), Alcalá de Henares, Madrid, p. 230.
- AEMET/IPMA, 2011. Atlas Climático Ibérico/Iberian Climate Atlas. Agencia Estatal de Meteorología (AEMET) and Instituto Português do Mar e da Atmosfera (IPMA), Madrid. <http://www.aemet.es/es/divulgacion/publicaciones/>.
- Akçar, N., 2022. The anatolian mountains: glacial landforms from the last glacial maximum. In: Palacios, D., Hughes, P.D., García-Ruiz, J.M., Andrés, N. (Eds.), *European Glacial Landscapes: Maximum Extent of Glaciations*. Elsevier, pp. 497–504. <https://doi.org/10.1016/B978-0-12-823498-3.00016-9>.
- Akçar, N., 2023. The Anatolian Mountains: glacial landforms during deglaciation. In: Palacios, D., Hughes, P.D., García-Ruiz, J.M., Andrés, N. (Eds.), *European Glacial Landscapes: Last Deglaciation*. Elsevier, pp. 233–239. <https://doi.org/10.1016/B978-0-323-91899-2.00011-5>.
- Akçar, N., Ivy-Ochs, S., Kubik, P.W., Schlüchter, C., 2011. Post-depositional impacts on 'Findlinge' (erratic boulders) and their implications for surface-exposure dating. *Swiss J. Geosci.* 104, 445–453. <https://doi.org/10.1007/s00015-011-0088-7>.
- Alcalá-Reygosa, J., Palacios, D., Campos, N., de Andrés, N., Schimmelpennig, I., Léanni, L., Sanjurjo, J., Aster Team., 2019. The rapid deglaciation of the la Vega gorge following the Last Glacial Maximum. Abstract Book for INQUA 2019, Dublin, Ireland, p. 1888. P-2443. <http://iqua.ie/wp-content/uploads/2020/02/INQUA-2019-Abstract-book.pdf>.
- Allard, J.L., 2022. Pleistocene Glaciation in the Mediterranean: Extent, Timing and Climatic Significance. A thesis submitted to The University of Manchester for the degree of Doctor of Philosophy in the Faculty of Humanities. <https://doi.org/10.13140/RG.2.2.22570.29126>.
- Allard, J.L., Hughes, P.D., Woodward, J.C., 2021. Heinrich Stadial aridity forced Mediterranean-wide glacier retreat in the last cold stage. *Nat. Geosci.* 14, 197–205. <https://doi.org/10.1038/s41561-021-00703-6>.
- Alonso-González, E., López-Moreno, J.I., Navarro-Serrano, F.M., Revuelto, J., 2020. Impact of North Atlantic oscillation on the snowpack in iberian peninsula mountains. *Water* 12 (1), 105. <https://doi.org/10.3390/w12010105>.
- Ancorenaz, A., Braucher, R., Defive, E., Poiraud, A., Steiger, J., 2022. Last glacial fluctuations in the southwestern Massif Central, Aubrac (France): first direct chronology from cosmogenic <sup>10</sup>Be and <sup>26</sup>Al exposure dating. *Quat. Sci. Rev.* 285, 107500. <https://doi.org/10.1016/j.quascirev.2022.107500>.
- Andrés, N., Gómez-Ortiz, A., Fernández-Fernández, J.M., Tanarro, L.M., Salvador, F., Oliva, M., Palacios, D., 2018. Timing of deglaciation and rock glacier origin in the southeastern Pyrenees: a review and new data. *Boreas* 47, 1050–1071. <https://doi.org/10.1111/bor.12324>.
- Antunes, B., Velo-Antón, G., Buckley, D., Pereira, R.J., Martínez-Solano, I., 2021. Physical and ecological isolation contribute to maintain genetic differentiation between fire salamander subspecies. *Heredity* 126, 776–789. <https://doi.org/10.1038/s41437-021-00405-0>.
- Balco, G., Stone, J.O., Lifton, N.A., Dunai, T.J., 2008. A complete and easily accessible means of calculating surface exposure ages or erosion rates from <sup>10</sup>Be and <sup>26</sup>Al measurements. *Quat. Geochronol.* 3, 174–195. <https://doi.org/10.1016/j.quageo.2007.12.001>.
- Barker, S., Diz, P., Vautravers, M.J., Pike, J., Knorr, G., Hall, I.R., Broecker, W.S., 2009. Interhemispheric Atlantic seesaw response during the last deglaciation. *Nature* 457 (7233), 1097–1102. <https://doi.org/10.1038/nature07770>.
- Barr, I.D., Clark, C.H., 2012. Late Quaternary glaciations in Far NE Russia; combining moraines, topography and chronology to assess regional and global glaciation synchrony. *Quat. Sci. Rev.* 53, 72–87. <https://doi.org/10.1016/j.quascirev.2012.08.004>.
- Barr, I.D., Lovell, H., 2014. A review of topographic controls on moraine distribution. *Geomorphology* 226, 44–64. <https://doi.org/10.1016/j.geomorph.2014.07.030>.
- Batchelor, C.L., Margold, M., Krapp, M., Murton, D.K., Dalton, A.S., Gibbard, P.L., Stokes, C.R., Murton, J.B., Manica, A., 2019. The configuration of Northern Hemisphere ice sheets through the Quaternary. *Nat. Commun.* 10, 1–10. <https://doi.org/10.1038/s41467-019-11601-2>.
- Baykal, Y., Stevens, T., Bateman, M.D., Pfaff, K., Sechi, D., Banak, A., Suica, S., Zhang, H., Nie, J., 2022. Eurasian Ice Sheet derived meltwater pulses and their role in driving atmospheric dust activity: late Quaternary loess sources in SE England. *Quat. Sci. Rev.* 296, 107804. <https://doi.org/10.1016/j.quascirev.2022.107804>.
- Beghin, P., Charbit, S., Kageyama, M., Combourieu-Nebout, N., Hatté, C., Dumas, C., Peterschmitt, J.Y., 2016. What drives LGM precipitation over the western Mediterranean? A study focused on the Iberian Peninsula and northern Morocco. *Clim. Dynam.* 46, 2611–2631. <https://doi.org/10.1007/s00382-015-2720-0>.
- Bereiter, B., Shackleton, S., Baggenstos, D., Kawamura, K., Severinghaus, J., 2018. Mean global ocean temperatures during the last glacial transition. *Nature* 553 (7686), 39–44. <https://doi.org/10.1038/nature25152>.
- Blain, H.A., Rubio-Jara, S., Panera, J., Uribelarrea, D., Laplana, C., Herráez, E., Pérez-González, A., 2017. A new middle pleistocene (marine oxygen isotope stage 6) cold herpetofaunal assemblage from the central iberian peninsula (manzanares valley, madrid). *Quat. Res.* 87, 499–515. <https://doi.org/10.1017/qua.2017.17>.
- Bordonau, J., Vilaplana, J.M., Fontugne, M., 1993. The glaciolacustrine complex of Llestui (Central Southern Pyrenees): a key-locality for the chronology of the last glacial cycle in the Pyrenees. *C. R. Acad. Sci. Paris* 316 (II), 807–813.
- Böse, M., Lüthgens, C., Lee, J.R., Rose, J., 2012. Quaternary glaciations of northern Europe. *Quat. Sci. Rev.* 44, 1–25. <https://doi.org/10.1016/j.quascirev.2012.04.017>.
- Boston, C.M., Lukas, S., 2019. Topographic controls on plateau icefield recession: insights from the younger dryas monadlihi icefield, scotland. *J. Quat. Sci.* 34 (6), 433–451. <https://doi.org/10.1002/jqs.3111>.
- Bullón, T., 2016. The upper Pleistocene on the northern face of the Guadarrama Mountains (central Spain): palaeoclimatic phases and glacial activity. *Geomorphology* 268, 233–245. <https://doi.org/10.1016/j.geomorph.2016.06.015>.
- Butzer, K.W., Fränze, O., 1959. Observations on pre-würm glaciation of the iberian peninsula. *Zeitschrift für Geomorphol.* NF 3, 85–97.
- Calvet, M., Delmas, M., Gunnell, Y., Braucher, R., Bourlès, D., 2011. Recent advances in research on quaternary glaciations in the Pyrenees. In: Ehlers, J., Gibbard, P.L., Hughes, P.D. (Eds.), *Quaternary Glaciations-Extent and Chronology. A Closer Look*. Developments in Quaternary Science, Volume 15. Elsevier, pp. 127–139. <https://doi.org/10.1016/B978-0-444-53447-7.00011-8> (Chapter 11).
- Campos, N., Tanarro, L.M., Palacios, D., 2018. Geomorphology of glaciated gorges in a granitic massif (Gredos range, central Spain). *J. Maps* 14 (2), 321–329. <https://doi.org/10.1080/17445647.2018.1468829>.
- Carrasco, R.M., 1997. Estudio Geomorfológico del Valle del Jerte (Sistema Central Español): secuencia de procesos y dinámica morfológica actual. Complutense Univ. Madrid, Spain. Ph.D. Thesis.
- Carrasco, R.M., Pedraza, J., Domínguez-Villar, D., Willenbring, J.K., Villa, J., 2011a. The plateau glaciers in the Sierra de Gredos during the last glacial period. XVIII INQUA Congress, 21st–27th July 2011, Bern, Switzerland, Communication. Abstract in: *Quat. Int.* 279–280 (2012), 81. <https://doi.org/10.1016/j.quaint.2012.07.357>.

- Carrasco, R.M., Pedraza, J., Razola, L., Domínguez-Villar, D., Willenbring, J.K., Ruiz-Zapata, B., 2011b. Typologies of genetic tills in the Sierra de Gredos (Spanish central system). XVIII INQUA congress, 21st–27th July 2011, Bern, Switzerland, posters. Abstract in. *Quat. Int.* 279–280 (2012), 81. <https://doi.org/10.1016/j.quaint.2012.07.358>.
- Carrasco, R.M., Pedraza, J., Domínguez-Villar, D., Villa, J., Willenbring, J.K., 2013a. The plateau glacier in the Sierra de Bejar (Iberian Central System) during its maximum extent. Reconstruction and chronology. *Geomorphology* 196, 83–93. <https://doi.org/10.1016/j.geomorph.2012.03.019>.
- Carrasco, R.M., Pedraza, J., Domínguez-Villar, D., Willenbring, J.K., Villa, J., 2013b. Supraglacial debris supply in the Cuerpo de Hombre paleoglaciar (Spanish Central System). Reconstruction and interpretation of a rock avalanche event. *Geogr. Ann. Ser. A Phys. Geogr.* 95, 211–266. <https://doi.org/10.1111/geoa.12010>.
- Carrasco, R.M., Pedraza, J., Domínguez-Villar, D., Willenbring, J.K., Villa, J., 2015. Sequence and chronology of the Cuerpo de Hombre paleoglaciar (Iberian Central System) during the last glacial cycle. *Quat. Sci. Rev.* 129, 163–177. <https://doi.org/10.1016/j.quascirev.2015.09.021>.
- Carrasco, R.M., Pedraza, J., Willenbring, J.K., Karampaglidis, T., Soteres, R.L., Martín-Duque, J.F., 2016. Morfología glacial del Macizo de Los Pelados-El Nevero (Parque Nacional de la Sierra de Guadarrama). Nueva interpretación y cronología. *Boletín de la Real Sociedad Española de Historia Natural. Sección Geología* 110, 49–66. <http://www.rsehn.es/index.php?d=publicaciones&num=61&w=362&f=1>.
- Carrasco, R.M., Turu, V., Pedraza, J., Muñoz-Martín, A., Ros, X., Sánchez, J., Ruiz-Zapata, B., Olaiz, A.J., Herrero-Simón, R., 2018. Near surface geophysical analysis of the Navamuño depression (Sierra de Béjar, Iberian Central System): geometry, sedimentary infill and genetic implications of tectonic and glacial footprint. *Geomorphology* 315, 1–16. <https://doi.org/10.1016/j.geomorph.2018.05.003>.
- Carrasco, R.M., Soteres, R.S., Pedraza, J., Fernández-Lozano, J., Turu, V., López-Sáez, J.A., Karampaglidis, T., Granja-Bruña, J.L., Muñoz-Martín, A., 2020. Glacial geomorphology of the high Gredos massif: Gredos and pinar valleys (Iberian central system, Spain). *J. Maps* 16 (2), 790–804. <https://doi.org/10.1080/17445647.2020.1833768>.
- Carrasco, R.M., Pedraza, J., Palacios, D., 2022a. The glaciers of the Sierra de Gredos. In: Oliva, M., Palacios, D., Fernández-Fernández, J.M. (Eds.), *Iberia, Land of Glaciers*. Elsevier, Amsterdam, Netherlands, pp. 457–483. <https://doi.org/10.1016/B978-0-12-821941-6.00022-0> (Chapter 4).18.
- Carrasco, R.M., Pedraza, J., Palacios, D., 2022b. The glaciers of the sierras de Guadarrama and Somosierra. In: Oliva, M., Palacios, D., Fernández-Fernández, J.M. (Eds.), *Iberia, Land of Glaciers*. Elsevier, Amsterdam, Netherlands, pp. 485–503. <https://doi.org/10.1016/B978-0-12-821941-6.00023-2> (Chapter 4).19.
- Chandler, B., Lovell, H., Boston, C., Lukas, S., Barr, I.D., Benediktsson, Í.Ö., Benn, D.I., Clark, C.D., Darvill, C.M., Evans, D.J.A., Ewertowski, M.W., Loibl, D., Margold, M., Otto, J.C., Roberts, D.H., Stokes, C.R., Storrar, R.D., Stroeven, A.P., 2018. Glacial geomorphological mapping: a review of approaches and frameworks for best practice. *Earth Sci. Rev.* 185, 806–846. <https://doi.org/10.1016/j.earscirev.2018.07.015>.
- Cheng, H., Edwards, R.L., Sinha, A., Spötl, C., Yi, L., Chen, S., Kelly, M., Kathayat, G., Wang, X., Li, X., Kong, X., Wang, Y., Ning, Y., Zhang, H., 2016. The Asian monsoon over the past 640,000 years and ice age terminations. *Nature* 534 (7609), 640–646. <https://doi.org/10.1038/nature18591>.
- Clapperton, C.M., 1993. *Quaternary Geology and Geomorphology of South America*. Elsevier, New York, p. 779.
- Clapperton, C., 1995. Fluctuations of local glaciers at the termination of the Pleistocene: 18–8 ka BP. *Quat. Int.* 28, 41–50. [https://doi.org/10.1016/1040-6182\(95\)00041-G](https://doi.org/10.1016/1040-6182(95)00041-G).
- Clark, P.U., Dyke, A.S., Shakun, J.D., Carlson, A.E., Clark, J., Wohlfarth, B., et al., 2009. The last glacial maximum. *Science* 325 (5941), 710–714. <https://doi.org/10.1126/science.1172873>.
- Clark, P.U., Shakun, J.D., Baker, P.A., Patrick, J., Bartlein, P.J., Brewere, S., et al., 2012. Global climate evolution during the last deglaciation. *Proc. Natl. Acad. Sci. USA* 109 (19), E1134–E1142. <https://doi.org/10.1073/pnas.111661910>.
- Clark, C.D., Ely, J.C., Hindmarsh, R.C.A., Bradley, S., Igneczi, A., Fabel, D., Ó Cofaigh, C., Chiverrell, R.C., Scours, J., Benetti, S., Bradwell, T., Evans, D.J.A., Roberts, D.H., Burke, M., Callard, S.L., Medialdea, A., Saher, M., Small, D., Smedley, R.K., Gasson, E., Gregoire, L., Gandy, N., Hughes, A.L.C., Ballantyne, C., Bateman, M.D., Bigg, G.R., Doole, J., Dove, D., Duller, G.A.T., Jenkins, G.T.H., Livingstone, S.L., McCarron, S., Moreton, S., Pollard, D., Praeg, D., Sejrup, H.P., van Landeghem, K.J.J., Wilson, P., 2022. Growth and retreat of the last British–Irish Ice Sheet, 31 000 to 15 000 years ago: the BRITICE-CHRONO reconstruction. *Boreas*. <https://doi.org/10.1111/bor.12594>.
- Coleman, C.G., Carr, S.J., Parker, A.G., 2009. Modelling topoclimatic controls on palaeoglaciers: implications for inferring palaeoclimate from geomorphic evidence. *Quat. Sci. Rev.* 28, 249–259. <https://doi.org/10.1016/j.quascirev.2008.10.016>.
- Cossart, É., Braucher, R., Fort, M., Bourlès, D.L., Carcaillet, J., 2008. Slope instability in relation to glacial debuiting in alpine areas (upper durance catchment, southeastern France): evidence from field data and <sup>10</sup>Be cosmic ray exposure ages. *Geomorphology* 95, 3–26. <https://doi.org/10.1016/j.geomorph.2006.12.022>.
- Cowton, T., Hughes, P.D., Gibbard, P.L., 2009. Palaeoglaciation of parque natural lago de Sanabria, northwest Spain. *Geomorphology* 108, 282–291.
- Davies, B.J., Thorndyraft, V.R., Fabel, D., Martin, J.R.V., 2018. Asynchronous glacier dynamics during the antarctic cold reversal in central Patagonia. *Quat. Sci. Rev.* 200, 287–312. <https://doi.org/10.1016/j.quascirev.2018.09.025>.
- Davies, B., Bendle, J., Carrivick, J., McNabb, R., McNeil, C., Peltó, M., Campbell, S., Holt, T., Ely, J., Markle, B., 2022. Topographic controls on ice flow and recession for Juneau Icefield (Alaska/British Columbia). *Earth Surf. Process. Landforms* 47, 2357–2390. <https://doi.org/10.1002/esp.5383>.
- de Vicente, G., Cunha, P.P., Muñoz-Martín, A., Cloetingh, S.A.P.L., Olaiz, A., Vegas, R., 2018. The Spanish-Portuguese Central System: an example of intense intraplate deformation and strain partitioning. *Tectonics* 37, 4444–4469. <https://doi.org/10.1029/2018TC005204>.
- Delaney, I., Anderson, L.S., 2022. Debris cover limits subglacial erosion and promotes till accumulation. *Geophys. Res. Lett.* 49, e2022GL099049. <https://doi.org/10.1029/2022GL099049>.
- Delmas, M., 2015. The last maximum ice extent and subsequent deglaciation of the Pyrenees: an overview of recent research. *Cuadernos Invest. Geogr.* 41 (2), 359–387. <https://doi.org/10.18172/cig.2708>.
- Delmas, M., Gunnell, Y., Braucher, R., Calvet, M., Bourlès, D., 2008. Exposure age chronology of the last glaciation in the eastern Pyrenees. *Quat. Res.* 69, 231–241. <https://doi.org/10.1016/j.yqres.2007.11.004>.
- Delmas, M., Gunnell, Y., Calvet, M., Reixach, T., Oliva, M., 2022. The Pyrenees: glacial landforms prior to the last glacial maximum. In: Palacios, D., Hughes, P.D., García-Ruiz, J.M., Andrés, N. (Eds.), *European Glacial Landscapes: Maximum Extent of Glaciations*. Elsevier, pp. 295–307. <https://doi.org/10.1016/B978-0-12-823498-3.00020-0>.
- Delmas, M., Gunnell, Y., Calvet, M., Reixach, T., Oliva, M., 2023. The Iberian Mountains: glacial landforms during deglaciation. In: Palacios, D., Hughes, P.D., García-Ruiz, J.M., Andrés, N. (Eds.), *European Glacial Landscapes: Last Deglaciation*. Elsevier, pp. 185–200. <https://doi.org/10.1016/B978-0-323-91899-2.00040-1>.
- Demek, J. (Ed.), 1972. *Manual of Detailed Geomorphological Mapping*. In: IGU Commission for Geomorphological Mapping, Academia, Prague.
- Denton, G.H., Anderson, R.F., Toggweiler, J.R., Edwards, R.L., Schaefer, J.M., Putnam, A.E., 2010. The Last Glacial Termination. *Science* 328, 1652–1656. <https://doi.org/10.1126/science.1184119>.
- Domínguez-Villar, D., Carrasco, R.M., Pedraza, J., Cheng, H., Edwards, R.L., Willenbring, J.K., 2013. Early maximum extent of paleoglaciers from Mediterranean mountains during the last glaciation. *Sci. Rep.* 3, 2034. <https://www.nature.com/articles/srep02034>.
- Dortch, J.M., Owen, L.A., Caffee, M.W., 2013. Timing and climatic drivers for glaciation across semi-arid western Himalayan-Tibetan orogen. *Quat. Sci. Rev.* 78, 188–208. <https://doi.org/10.1016/j.quascirev.2013.07.025>.
- Doughty, A.L., Kaplan, M.R., Peltier, C., Barker, S., 2021. A maximum in global glacier extent during MIS 4. *Quat. Sci. Rev.* 261, 106948. <https://doi.org/10.1016/j.quascirev.2021.106948>.
- Durán, I., Sánchez, E., Yagüe, C., 2013. Climatology of precipitation over the Iberian central system mountain range. *Int. J. Climatol.* 33, 2260–2273. <https://doi.org/10.1002/joc.3602>.
- Dyke, L.M., Hughes, A.L.C., Murray, T., Hiemstra, J.F., Andresen, C.S., Rodés, A., 2014. Evidence for the asynchronous retreat of large outlet glaciers in southeast Greenland at the end of the last glaciation. *Quat. Sci. Rev.* 99, 244–259. <https://doi.org/10.1016/j.quascirev.2014.06.001>.
- Ellis, R., Palmer, M., 2016. Modulation of ice ages via precession and dust-albedo feedbacks. *Geosci. Front.* 7, 891–909. <https://doi.org/10.1016/j.gsf.2016.04.004>.
- Engel, Z., Mentlík, P., Braucher, R., Minár, J., Léanni, L., Aster Team, 2015. Geomorphological evidence and 10Be exposure ages for the last glacial maximum and deglaciation of the veľká and malá studená dolina valleys in the high tatra mountains, central Europe. *Quat. Sci. Rev.* 124, 106–123. <https://doi.org/10.1016/j.quascirev.2015.07.015>.
- Evans, I.S., 1977. World-wide variations in the direction and concentration of cirque and glacier aspects. *Geogr. Ann.* 59A (3–4), 151–175. <https://doi.org/10.1080/04353676.1977.11879949>.
- Federici, P.R., Ribolini, A., Spagnolo, M., 2017. Glacial history of the Maritime Alps from the last glacial maximum to the little ice age. In: Hughes, P.D., Woodward, J.C. (Eds.), *Quaternary Glaciation in the Mediterranean Mountains*, vol. 433. Geological Society, London, Special Publications, pp. 137–159. <https://doi.org/10.1144/SP433.9>.
- Fernandes, M., Oliva, M., Vieira, G., 2020. Paraglacial slope failures in the aran valley (central Pyrenees). *Quat. Int.* 566 (567), 24–38. <https://doi.org/10.1016/j.quaint.2020.07.045>.
- FGDC, 2006. FGDC Digital Cartographic Standard for Geologic Map Symbolization. Federal Geographic Data Committee Document Number FGDC-STD-013-2006, 290 p., 2 plates. [https://ngmdb.usgs.gov/fgdc\\_gds/geolsymstd/fgdc-geolsym-all.pdf](https://ngmdb.usgs.gov/fgdc_gds/geolsymstd/fgdc-geolsym-all.pdf).
- Fletcher, W.J., Sánchez-Goni, M.F., 2008. Orbital- and sub-orbital-scale climate impacts on vegetation of the western Mediterranean basin over the last 48,000 yr. *Quat. Res.* 70, 451–464. <https://doi.org/10.1016/j.yqres.2008.07.002>.
- Florineth, D., Schlüchter, C., 2000. Alpine evidence for atmospheric circulation patterns in Europe during the last glacial maximum. *Quat. Res.* 54, 295–308. <https://doi.org/10.1006/qres.2000.2169>.
- Frochoso, M., González-Pellejero, R., Allende, F., 2013. Pleistocene glacial morphology and timing of Last Glacial Cycle in Cantabrian Mountains (Northern Spain): new chronological data from the Asón area. *Cent. Eur. J. Geosci.* 5, 12–27. <https://doi.org/10.2478/s13533-012-0117-8>.
- García-Antón, M., Génova, M., Postigo-Mijarra, J.M., García-Álvarez, S., Morla, C., García-Amorena, I., 2021. Holocene woodland history of the Sierra de Ayllón (central Spain). *Veg. Hist. Archaeobotany* 30, 331–346. <https://doi.org/10.1007/s00334-020-00787-x>.

- García-Ruiz, J.M., Valero, B., Martí-Bono, C.E., González-Samperiz, P., 2003. Asynchrony of maximum glacier advances in the central Spanish Pyrenees. *J. Quat. Sci.* 18, 61–72.
- García-Ruiz, J.M., Moreno, A., González-Samperiz, P., Valero-Garcés, B., Martí-Bono, C., 2010. La cronología del último ciclo glaciar en las montañas del sur de Europa. *Una revisión*. *Cuaternario Geomorfol.* 24, 35–46.
- García-Ruiz, J.M., Serrano, E., 2022. The glaciers of the central-western Pyrenees. In: Oliva, M., Palacios, D., Fernández-Fernández, J.M. (Eds.), *Iberia, Land of Glaciers*. Elsevier, Amsterdam, Netherlands, pp. 123–155. <https://doi.org/10.1016/B978-0-12-821941-6.00007-4> (Chapter 4).
- García-Sancho, L., Palacios, D., Marcos, J., Valladares, F., 2001. Geomorphological significance of lichen colonization in a present snow hollow: Hoya del Cuchillar de las Navajas, Sierra de Gredos (Spain). *Catena* 43 (4), 323–340. [https://doi.org/10.1016/S0341-8162\(00\)00131-4](https://doi.org/10.1016/S0341-8162(00)00131-4).
- GEODE, 2004. Cartografía Geológica Digital Continua a Escala 1:50.000. Instituto Geológico y Minero de España (IGME). <http://info.igme.es/cartografiadigital/geologica/Geode.aspx>.
- Gildor, H., Ashkenazy, Y., Tziperman, E., Lev, I., 2014. The role of sea ice in the temperature-precipitation feedback of glacial cycles. *Clim. Dynam.* 43 (3–4), 1001–1010. <https://doi.org/10.1007/s00382-013-1990-7>.
- Gil-García, M.J., Ruiz-Zapata, M.B., Rubio-Jara, S., Panera, J., Pérez-González, A., 2019. Landscape evolution during the middle and late pleistocene in the Madrid basin (Spain): vegetation dynamics and human activity in the Jarama-Manzanares rivers (Madrid) during the Pleistocene. *Quat. Int.* 520, 39–48. <https://doi.org/10.1016/j.quaint.2018.02.034>.
- Gillespie, A., Molnar, P., 1995. Asynchronous maximum advances of mountain and continental glaciers. *Rev. Geophys.* 33, 311–364. <https://doi.org/10.1029/95RG00995>.
- Giraudi, C., 2015. The upper Pleistocene deglaciation on the Apennines (peninsular Italy). *Cuadernos de Investigación Geográfica* 41 (2), 337–358. <https://doi.org/10.18172/cig.2696>.
- Giraudi, C., Frezzotti, M., 1997. Late Pleistocene glacial events in the central Apennines, Italy. *Quat. Res.* 48, 280–290. <https://doi.org/10.1006/qres.1997.1928>.
- Glasser, N.F., Harrison, S., Jansson, K.N., 2009. Topographic controls on glacier sediment–landform associations around the temperate North Patagonian Icefield. *Quat. Sci. Rev.* 28, 2817–2832. <https://doi.org/10.1016/j.quascirev.2009.07.011>.
- Gómez-Ortiz, A., Palacios, P., Palade, B., Vázquez-Selem, L., Salvador-Franch, F., 2012. The deglaciation of the Sierra Nevada (southern Spain). *Geomorphology* 159–160, 93–105. <https://doi.org/10.1016/j.geomorph.2012.03.008>.
- Gómez-Ortiz, A., Oliva, M., Palacios, D., Salvador Franch, F., Vázquez Selem, L., Salvá-Catarineu, M., de Andrés, N., 2015. The deglaciation of Sierra Nevada (Spain), synthesis of the knowledge and new contributions. *Cuadernos de Investigación Geográfica* 41 (2), 409–426. <https://doi.org/10.18172/cig.2722>.
- Gómez-Ortiz, A., Oliva, M., Palacios, D., Salvador-Franch, F., 2022. The glaciers of the Sierra Nevada. In: Oliva, M., Palacios, D., Fernández-Fernández, J.M. (Eds.), *Iberia, Land of Glaciers*. Elsevier, Amsterdam, Netherlands, pp. 505–524. <https://doi.org/10.1016/B978-0-12-821941-6.00024-4> (Chapter 4).
- González-Martín, J.A., Pellicer-Corellano, F., 1988. Rasgos generales del periglaciario de la Península Ibérica. II. Dominio continental de las tierras interiores. *Cuadernos de Investigación Geográfica* 14 (1–2), 23–80. <https://dialnet.unirioja.es/servlet/articulo?codigo=81466>.
- González-Sampériz, P., Leroy, S.A.G., Carrión, J.S., Fernández, S., García-Antón, M., Gil-García, M.J., Uzquiano, P., Valero-Garcés, B., Figueiral, I., 2010. Steppes, savannahs, forests and phytodiversity reservoirs during the Pleistocene in the Iberian Peninsula. *Rev. Palaeobot. Palynol.* 162, 427–457. <https://doi.org/10.1016/j.revpalbo.2010.03.009>.
- Grämiger, L.M., Moore, J.R., Gischig, V.S., Ivy-Ochs, S., Loew, S., 2017. Beyond debuiting: mechanics of paraglacial rock slope damage during repeat glacial cycles. *J. Geophys. Res. Earth Surf.* 122, 1004–1036. <https://doi.org/10.1002/2016JF003967>.
- Granja-Bruña, J.L., Turu, V., Carrasco, R.M., Muñoz-Martín, A., Ros, X., Fernández-Lozano, J., Soteres, R.L., Karampaglidis, T., López-Sáez, J.A., Pedraza, J., 2021. Geophysical characterization of the El Cervunal kame complex (Sierra de Gredos, Iberian Central System): insight of infill geometry and reconstruction of former glacial formations. *J. Appl. Geophys.* 195. <https://doi.org/10.1016/j.jappgeo.2021.104478>.
- Gribenski, N., Valla, P.G., Preusser, F., Roattino, T., Cruzet, C., Buoncristiani, J.-F., 2021. Out-of-phase Late Pleistocene glacial maxima in the Western Alps reflect past changes in North Atlantic atmospheric circulation. *Geology* 49 (9), 1096–1101. <https://doi.org/10.1130/G48688.1>.
- Hemming, S.R., 2004. Heinrich events: massive late Pleistocene detritus layers of the North Atlantic and their global climate imprint. *Rev. Geophys.* 42, RG1005. <https://doi.org/10.1029/2003RG000128>.
- Hernández, A., Sáez, A., Santos, R.N., Rodrigues, T., Martín-Puertas, C., Gil-Romera, G., Abbott, M., Carballeira, R., Costa, P., Giral, S., Gomes, S.D., Grifone, M., Ibañez-Insa, J., Leira, M., Moreno, J., Naughton, F., Oliveira, D., Raposo, P.M., Trigo, R.M., Vieira, G., Ramos, A.M., 2023. The timing of the deglaciation in the Atlantic Iberian mountains: insights from the stratigraphic analysis of a lake sequence in Serra da Estrela (Portugal). *Earth Surf. Process. Landforms* 48 (2), 233–242. <https://doi.org/10.1002/esp.5536>.
- Houmark-Nielsen, M., 2010. Extent, age and dynamics of marine isotope stage 3 glaciations in the southwestern baltic basin. *Boreas* 39, 343–359. <https://doi.org/10.1111/j.1502-3885.2009.00136.x>.
- Hughes, A.L.C., Gyllencreutz, R., Lohne, O.S., Mangerud, J., Svendsen, J.I., 2016. The last Eurasian ice sheets – a chronological database and time-slice reconstruction, DATED-1. *Boreas* 45, 1–45. <https://doi.org/10.1111/bor.12142>.
- Hughes, A.L.C., Winsborrow, M.C., Greenwood, S.L., 2022b. European ice sheet complex evolution during the last glacial maximum (29–19 ka). In: Palacios, D., Hughes, P.D., García-Ruiz, J.M., Andrés, N. (Eds.), *European Glacial Landscapes: Maximum Extent of Glaciations*. Elsevier, pp. 361–372. <https://doi.org/10.1016/B978-0-12-823498-3.00038-8>.
- Hughes, P.D., 2022. Concept and global context of the glacial landforms from the Last Glacial Maximum. In: Palacios, D., Hughes, P.D., García-Ruiz, J.M., Andrés, N. (Eds.), *European Glacial Landscapes: Maximum Extent of Glaciations*. Elsevier, pp. 355–358. <https://doi.org/10.1016/B978-0-12-823498-3.00039-X>.
- Hughes, P.D., Woodward, J.C., Gibbard, P.L., 2006a. Late Pleistocene glaciers and climate in the Mediterranean region. *Global Planet. Change* 50, 83–98. <https://doi.org/10.1016/j.gloplacha.2005.07.005>.
- Hughes, P.D., Woodward, J.C., Gibbard, P.L., Macklin, M., Gilmour, M., Smith, G., 2006b. The glacial history of the Pindus mountains, Greece. *J. Geol.* 114, 413–434. <https://doi.org/10.1086/504177>.
- Hughes, P.D., Woodward, J.C., 2008. Timing of glaciation in the Mediterranean mountains during the last cold stage. *J. Quat. Sci.* 23, 575–588. <https://doi.org/10.1002/jqs.1212>.
- Hughes, P.D., Gibbard, P.L., Ehlers, J., 2013. Timing of glaciation during the last glacial cycle: evaluating the concept of a global ‘Last Glacial Maximum’ (LGM). *Earth Sci. Rev.* 125, 171–198. <https://doi.org/10.1016/j.earscirev.2013.07.003>.
- Hughes, P.D., Gibbard, P.L., 2015. A stratigraphical basis for the last glacial maximum (LGM). *Quat. Int.* 383, 174–185. <https://doi.org/10.1016/j.quaint.2014.06.006>.
- Hughes, P.D., Woodward, J.C., 2017. Quaternary glaciation in the Mediterranean mountains: a new synthesis. In: Hughes, P.D., Woodward, J.C. (Eds.), *Quaternary Glaciation in the Mediterranean Mountains*, vol. 433. Geological Society of London, pp. 1–23. <https://doi.org/10.1144/SP433.14>.
- Hughes, P.D., Gibbard, P.L., Ehlers, J., 2020. The “missing glaciations” of the Middle Pleistocene. *Quat. Res.* 96, 161–183. <https://doi.org/10.1017/qua.2019.76>.
- Hughes, P.D., Allard, J.L., Woodward, J.C., 2022a. The Balkans: glacial landforms prior to the last glacial maximum. In: Palacios, D., Hughes, P.D., García-Ruiz, J.M., Andrés, N. (Eds.), *European Glacial Landscapes: Maximum Extent of Glaciations*. Elsevier, pp. 323–332. <https://doi.org/10.1016/B978-0-12-823498-3.00034-0>.
- Hughes, P.D., Allard, J.L., Woodward, J.C., 2023. The Balkans: glacial landforms during deglaciation. In: Palacios, D., Hughes, P.D., García-Ruiz, J.M., Andrés, N. (Eds.), *European Glacial Landscapes: Last Deglaciation*. Elsevier, pp. 221–231. <https://doi.org/10.1016/B978-0-323-91899-2.00055-3>.
- Ivy-Ochs, S., 2015. Glacier variations in the European Alps at the end of the last glaciation. *Cuadernos de Investigación Geográfica* 41 (2), 295–315. <https://doi.org/10.18172/cig.2750>.
- Ivy-Ochs, S., Kerschner, H., Reuther, A., Preusser, F., Heine, K., Maisch, M., Kubik, P.W., Schlüchter, C., 2008. Chronology of the last glacial cycle in the European Alps. *J. Quat. Sci.* 23, 559–573. <https://doi.org/10.1002/jqs.1202>.
- Ivy-Ochs, S., Monegato, G., Reitner, J.M., 2022. The Alps: glacial landforms from the last glacial maximum. In: Palacios, D., Hughes, P.D., García-Ruiz, J.M., Andrés, N. (Eds.), *European Glacial Landscapes: Maximum Extent of Glaciations*. Elsevier, pp. 449–460. <https://doi.org/10.1016/B978-0-12-823498-3.00030-3>.
- Ivy-Ochs, S., Monegato, G., Reitner, J.M., 2023. The Alps: glacial landforms during the deglaciation (18.9146 ka). In: Palacios, D., Hughes, P.D., García-Ruiz, J.M., Andrés, N. (Eds.), *European Glacial Landscapes: The Last Deglaciation*. Elsevier, pp. 175–183. <https://www.sciencedirect.com/science/article/pii/B978032391899200005X>.
- Jalut, G., Turu i Michels, V., Debouat, J.J., Otto, T., Ezquerro, J., Fontugne, M., Belet, J.M., Bonnet, L., Garcia de Celis, G., Redondo-Vega, J.M., Vidal-Romani, J.R., Santos, L., 2010. Paleoenvironmental studies in NW Iberia (Cantabrian range): vegetation history and synthetic approach of the last deglaciation phases in the western Mediterranean. *Palaeogeogr. Palaeoclimatol. Palaeoecol.* 297, 330–350. <https://doi.org/10.1016/j.palaeo.2010.08.012>.
- Jiménez-Sánchez, M., Farias, P., 2002. New radiometric and geomorphologic evidence of Last Glacial maximum older than 18 ka in SW European mountains: the example of Redes natural park, Cantabrian Mountains, NW Spain. *Geodin. Acta* 15, 93–101. [https://doi.org/10.1016/S0985-3111\(01\)01081-6](https://doi.org/10.1016/S0985-3111(01)01081-6).
- Jiménez-Sánchez, M., Rodríguez-Rodríguez, L., García-Ruiz, J.M., Domínguez-Cuesta, M.J., Farias, P., Valero-Garcés, B., Moreno, A., Rico, M., Valcárcel, M., 2013. A review of glacial geomorphology and chronology in northern Spain: timing and regional variability during the last glacial cycle. *Geomorphology* 196, 50–64. <https://doi.org/10.1016/j.geomorph.2012.06.009>.
- Kamleitner, S., Ivy-Ochs, S., Monegato, G., Gianotti, F., Akçar, N., Vockenhuber, C., Christl, M., Synal, H.-A., 2022. The ticino-toce glacier system (Swiss-Italian Alps) in the framework of the alpine last glacial maximum. *Quat. Sci. Rev.* 279, 107400. <https://doi.org/10.1016/j.quascirev.2022.107400>.
- Kamleitner, S., Ivy-Ochs, S., Manatschal, A., Akçar, N., Christl, M., Vockenhuber, C., Hadas, L., Synal, H.A., 2023. Last Glacial Maximum glacial fluctuations on the northern Alpine foreland: geomorphological and chronological reconstructions from the Rhine and Reuss glacier systems. *Geomorphology*, 108548. <https://doi.org/10.1016/j.geomorph.2022.108548>.
- Kaplan, M.R., Hein, A.S., Hubbard, A., Lax, S.M., 2009. Can glacial erosion limit the extent of glaciation? *Geomorphology* 103, 172–179. <https://doi.org/10.1016/j.geomorph.2008.04.020>.
- Kaushik, S., Ravanel, L., Magnin, F., Yan, Y., Trouve, E., Cusicanqui, D., 2022. Effects of topographic and meteorological parameters on the surface area loss of ice aprons in the Mont Blanc massif (European Alps). *Cryosphere* 16, 4251–4271. <https://doi.org/10.5194/tc-16-4251-2022>, 2022.

- Khandsuren, P., Seong, Y.B., Rhee, H.H., Lee, C.H., Sarikaya, M.A., Oh, J.S., Sandag, K., Yu, B.Y., 2022. Asynchronous Glacial Extent during the Last Glacial Maximum in the Bogd Massif of Gobi-Altay Range, Southwestern Mongolia: Aspect Control on Glacier Mass Balance. *The Cryosphere Discussion*. <https://doi.org/10.5194/tc-2022-238>. Preprint tc-2022-238.
- Lambeck, K., Purcell, A., Zhao, J., Svensson, N.-O., 2010. The Scandinavian ice sheet: from MIS 4 to the end of the last glacial maximum. *Boreas* 39, 410–435. <https://doi.org/10.1111/j.1502-3885.2010.00140.x>.
- Lambeck, K., Rouby, H., Purcell, A., Sun, Y., Sambridge, M., 2014. Sea level and global ice volumes from the last glacial maximum to the Holocene. *Proc. Natl. Acad. Sci. USA* 111, 15296–15303. <https://doi.org/10.1073/pnas.1411762111>.
- Larsen, N.K., Knudsen, K.L., Krohn, C.F., Kronborg, C., Murray, A.S., Nielsen, O.B., 2009. Late Quaternary ice sheet, lake and sea history of southwest Scandinavia – a synthesis. *Boreas* 38, 732–761. <https://doi.org/10.1111/j.1502-3885.2009.00101.x>.
- Leontaritis, A.D., 2021. *The Late Quaternary Glacial History of Greece*. Doctoral Thesis. Harokopio University of Athens, p. 194.
- Leontaritis, A.D., Pavlopoulos, K., Marrero, S.M., Ribolini, A., Hughes, P.D., Spagnolo, M., 2022. Glaciations on ophiolite terrain in the North Pindus Mountains, Greece: new geomorphological insights and preliminary <sup>36</sup>Cl exposure dating. *Geomorphology* 413, 108335. <https://doi.org/10.1016/j.geomorph.2022.108335>.
- Lifton, N., Sato, T., Dunai, T.J., 2014. Scaling in situ cosmogenic nuclide production rates using analytical approximations to atmospheric cosmic-ray fluxes. *Earth Planet. Sci. Lett.* 386, 149–160. <https://doi.org/10.1016/j.epsl.2013.10.052>.
- Liu, M., Shen, Y., González-Sampériz, P., Gil-Romera, G., ter Braak, C.J.F., Prentice, I.C., Harrison, S.P., 2023. Holocene climates of the Iberian Peninsula: pollen-based reconstructions of changes in the west–east gradient of temperature and moisture. *Clim. Past* 19, 803–834. <https://doi.org/10.5194/cp-19-803-2023>.
- López-Moreno, J.I., Vicente-Serrano, S.M., Morán-Tejeda, E., Lorenzo-Lacruz, J., Kenawy, A., Beni, M., 2011. Effects of the North Atlantic Oscillation (NAO) on combined temperature and precipitation winter modes in the Mediterranean mountains: observed relationships and projections for the 21st century. *Global Planet. Change* 77 (1–2), 62–76. <https://doi.org/10.1016/j.gloplacha.2011.03.003>.
- López-Moreno, J.I., Ceballos, J.L., Rojas-Heredia, F., Zabalza-Martínez, J., Vidaller, I., Revuelto, J., Alonso-González, E., Morán-Tejeda, E., García-Ruiz, J.M., 2020. Topographic control of glacier changes since the end of the little ice age in the Sierra Nevada de Santa Marta mountains, Colombia. *J. S. Am. Earth Sci.* 104, 102803. <https://doi.org/10.1016/j.jsames.2020.102803>.
- López-Sáez, J.A., Alba-Sánchez, F., Sánchez-Mata, D., Abel-Schaad, D., Gaviñán, R.G., Pérez-Díaz, S., 2015. A palynological approach to the study of *Quercus pyrenaica* forest communities in the Spanish Central System. *Phytocoenologia* 45 (1–2), 107–124. <https://doi.org/10.1127/0340-269X/2014/0044-0572>.
- López-Sáez, J.A., Carrasco, R.M., Turu, V., Ruiz-Zapata, B., Gil-García, M.J., Luellmo-Lautenschlaeger, R., Pérez-Díaz, S., Alba-Sánchez, F., Abel-Schaad, D., Ros, X., Pedraza, J., 2020. Late Glacial-early Holocene vegetation and environmental changes in the western Iberian Central System inferred from a key site: the Navamundo record, Béjar range (Spain). *Quat. Sci. Rev.* 230, 106167. <https://doi.org/10.1016/j.quascirev.2020.106167>.
- López-Sáez, J.A., Luellmo-Lautenschlaeger, R., Carrasco, R.M., Pedraza, J., Sánchez-Mata, D., Luengo-Nicolau, E., 2023. Diversity and conservation of the Gredos regional park peatlands (Iberian central system, Spain): geomorphological and geobotanical characterization and incoming threats. *Mediterranean Botany* 44, e80170. <https://doi.org/10.5209/mbot.80170>.
- Ludwig, P., Shao, Y., Kehl, M., Weniger, G.-C., 2018. The Last Glacial Maximum and Heinrich event I on the Iberian Peninsula: a regional climate modelling study for understanding human settlement patterns. *Global Planet. Change* 179, 34–47. <https://doi.org/10.1016/j.gloplacha.2018.08.006>.
- Makos, M., 2015. Deglaciation of the high tatra mountains. *Cuadernos Invest. Geogr.* 41 (2), 317–335. <https://doi.org/10.18172/cig.2697>.
- Makos, M., Dzierzek, J., Nitychoruk, J., Zreda, M., 2014. Timing of glacier advances and climate in the high tatra mountains (Western Carpathians) during the Last Glacial maximum. *Quat. Res.* 82, 1–13. <https://doi.org/10.1016/j.yqres.2014.04.001>.
- Makos, M., Rinterknecht, V., Braucher, R., Totoczko-Pasek, A., Arnold, M., Aumaître, G., Bourlés, D., Keddadouche, K., 2018. Last glacial maximum and lateglacial in the polish high tatra mountains - revised deglaciation chronology based on the <sup>10</sup>Be exposure age dating. *Quat. Sci. Rev.* 187, 130–156. <https://doi.org/10.1016/j.quascirev.2018.03.006>.
- Marcos, J., 2000. *Procesos actuales en el Alto Gredos: Garganta del Pinar*. In: En Peña, J.L., Sánchez-Fabre, M. y Lozano, M.V. (Eds.), *Procesos y formas periglaciares en la montaña mediterránea*. Instituto de Estudios Turolenses, Teruel, pp. 213–232.
- Marquette, G.C., Gray, J.T., Gosse, J.C., Courchesne, F., Stockli, L., Macpherson, G., Finkel, R., 2004. Felsenmeer persistence under non-erosive ice in the Torngat and Kaumajet mountains, Quebec and Labrador, as determined by soil weathering and cosmogenic nuclide exposure dating. *Can. J. Earth Sci.* 41, 19–38. <https://doi.org/10.1139/E03-072>.
- Martin, L., Bland, P.H., Balco, G., Lave, J., Delunel, R., Lifton, N., Laurent, V., 2017. The CREP program and the ICE-D production rate calibration database: a fully parameterizable and updated online tool to compute cosmic-ray exposure ages. *Quat. Geochronol.* 38, 25–49. <https://doi.org/10.1016/j.quageo.2016.11.006>.
- Martínez de Pisón, E., Muñoz Jiménez, J., 1972. Observaciones sobre la geomorfología del Alto Gredos. *Estud. Geográficos* 33 (129), 597–690.
- Martínez de Pisón, E., Palacios, D., 1997. Significado del episodio glacial en la evolución morfológica y en el paisaje de la Sierra de Gredos. *Sistema Central*. In: En Gómez Ortíz, A., y Pérez Alberti, A. (Eds.), *Las Huellas Glaciares de las Montañas Españolas*. Universidad de Santiago. Santiago de Compostela, pp. 163–207.
- Maslin, M., 2016. Forty years of linking orbits to ice ages. *Nature* 540, 208–209. <https://doi.org/10.1038/540208a>.
- McCull, S.T., Davies, T.R.H., McSaveney, M.J., 2010. Glacier retreat and rock-slope stability: de-bunking debulking. In: *Geologically Active: Delegate Papers 11th Congress of the International Association for Engineering Geology and the Environment*, Auckland, Aotearoa, 5–10 Septem-Ber 2010, pp. 467–474. Auckland, New Zealand.
- Mentlík, P., Engel, Z., Braucher, R., Léanni, L., Aster Team, 2013. Chronology of the late weichselian glaciation in the bohemian forest in central Europe. *Quat. Sci. Rev.* 65, 120–128. <https://doi.org/10.1016/j.quascirev.2013.01.020>.
- Mindrescu, M., Evans, I.S., Cox, N.J., 2010. Climatic implications of cirque distribution in the Romanian Carpathians: palaeowind directions during glacial periods. *J. Quat. Sci.* 25 (6), 875–888. <https://doi.org/10.1002/jqs.1363>.
- Mitchell, A.M., 1996. Significance of snowflow in the generation of loch lomond stadial (younger dryas) glaciers in the western pennines, northern england. *J. Quat. Sci.* 11 (3), 233–248. [https://doi.org/10.1002/\(SICI\)1099-1417\(1996/05/06\)11:3<233::AID-JQS240>3.0.CO;2-Q](https://doi.org/10.1002/(SICI)1099-1417(1996/05/06)11:3<233::AID-JQS240>3.0.CO;2-Q).
- Mix, A.C., Bard, E., Schneider, R., 2001. Environmental processes of the ice age: land, v oceans, glaciers (EPILOG). *Quat. Sci. Rev.* 20, 627–657. [https://doi.org/10.1016/S0277-3791\(00\)00145-1](https://doi.org/10.1016/S0277-3791(00)00145-1).
- Monegato, G., Kamleitner, S., Gianotti, F., Martin, S., Scapozza, C., Ivy-Ochs, S., 2022. The ticino-toce ice conveyor belts during the last glacial maximum. *Alpine and Mediterranean Quaternary* 35 (2), 119–134. <https://doi.org/10.26382/AMQ.2022.07>.
- Moreno, A., Valero-Garcés, B.L., Jiménez Sánchez, M., Domínguez, M.J., Mata, P., Navas, A., González-Sampériz, P., Stoll, H., Fariás, P., Morellón, M., Corella, P., Rico, M., 2010. The last deglaciation in the Picos de Europa national park (cantabrian mountains, northern Spain). *J. Quat. Sci.* 25 (7), 1076–1091. <https://doi.org/10.1002/jqs.1265>.
- Moreno-Arriba, J., 2010. *El Alto Tormes: Transformaciones Recientes en la Comarca de El Barco (Ávila) y Perspectivas de Desarrollo Sostenible en un Área de la Sierra de Gredos*. Tesis Doctoral en Geografía. UNED, Madrid. <http://e-spacio.uned.es/fez/eserv/tesisuned:GeoHis-jmoreno/Documento.pdf>.
- Muñoz, J., Palacios, D., Marcos, J., 1995. The influence of the geomorphologic heritage on present slope dynamics. The Gredos Cirque, Spain. *Pirineos* 145–146 (c), 35–63. <https://doi.org/10.3989/pirineos.1995.v145-146.146>.
- Muñoz-Salinas, E., Castillo, M., Sanderson, D., Kinnaird, T., 2013. Unravelling paraglacial activity on Sierra de Gredos, Central Spain: a study based on geomorphic markers, stratigraphy and OSL. *Catena* 110, 207–214. <https://doi.org/10.1016/j.catena.2013.06.018>.
- Naughton, F., Sánchez-Goni, M.F., Kageyama, M., Bard, E., Duprat, J., Cortijo, E., Desprat, S., Malaizé, B., Joly, C., Rostek, F., Turon, J.L., 2009. Wet to dry climatic trend in north-western Iberia within Heinrich events. *Earth Planet. Sci. Lett.* 284, 329–342. <https://doi.org/10.1016/j.epsl.2009.05.001>.
- Naughton, F., Sánchez-Goni, M.F., Rodrigues, T., Salgueiro, E., Costas, S., Desprat, S., Duprat, J., Michel, E., Rossignol, L., Zaragoza, S., Abrantes, F., 2016. Climate variability across the last deglaciation in NW Iberia and its margin. *Quat. Int.* 414, 9–22. <https://doi.org/10.1016/j.quaint.2015.08.073>.
- Naughton, F., Toucanne, S., Landais, A., Rodrigues, T., Vazquez-Riveiros, N., Sánchez Goni, M.F., 2023. The Heinrich stadial 1. In: Palacios, D., Hughes, P.D., García-Ruiz, J.M., Andrés, N. (Eds.), *European Glacial Landscapes: Last Deglaciation*. Elsevier, pp. 37–41. <https://doi.org/10.1016/B978-0-323-91899-2.00049-8>.
- Obermaier, H., Carandell, J., 1915. *Datos para la climatología cuaternaria en España*. *Bol. R. Soc. Esp. Hist. Nat.* 15, 402–411.
- Obermaier, H., Carandell, J., 1916. *Contribución al estudio del glaciario cuaternario de la Sierra de Gredos*. *Trabajos del Museo Nacional de Ciencias Naturales*. Ser. Geol. 14, 1–54.
- Oliva, M., Palacios, D., Fernández-Fernández, J.M., Rodríguez-Rodríguez, L., García-Ruiz, J.M., Andrés, N., Carrasco, R.M., Pedraza, J., Pérez-Alberti, A., Valcárcel, M., Hughes, P.D., 2019. Late quaternary glacial phases in the iberian peninsula. *Earth Sci. Rev.* 192, 564–600. <https://doi.org/10.1016/j.earscirev.2019.03.015>.
- Oliva, M., Palacios, D., Fernández-Fernández, J.M. (Eds.), 2022a. *Iberia, Land of Glaciers*. Elsevier, Amsterdam, Netherlands, p. 597.
- Oliva, M., Fernández-Fernández, J.M., Palacios, D., 2022b. The iberian mountains: glacial landforms from the last glacial maximum. In: Palacios, D., Hughes, P.D., García-Ruiz, J.M., Andrés, N. (Eds.), *European Glacial Landscapes*. Elsevier, pp. 473–480. <https://doi.org/10.1016/B978-0-12-823498-3.00029-7>.
- Oliva, M., Andrés, N., Fernández-Fernández, J.M., Palacios, D., 2023. The Iberian Mountains: glacial landforms during deglaciation. In: Palacios, D., Hughes, P.D., García-Ruiz, J.M., Andrés, N. (Eds.), *European Glacial Landscapes: Last Deglaciation*. Elsevier, pp. 201–208. <https://doi.org/10.1016/B978-0-323-91899-2.00043-7>.
- Ono, Y., Shulmeister, J., Lehmkühl, F., Asahi, K., Aoki, T., 2004. Timings and causes of glacial advances across the PEP-II transect (East-Asia to Antarctica) during the last glacial cycle. *Quat. Int.* 118–119, 55–68. [https://doi.org/10.1016/S1040-6182\(03\)00130-7](https://doi.org/10.1016/S1040-6182(03)00130-7).
- Palacios, D., García-Ruiz, J.M., 2015. Foreword: deglaciation in Europe. *New insights and questions*. *Cuadernos Invest. Geogr.* 41 (2), 257–259. <https://doi.org/10.18172/cig.2808>.
- Palacios, D., Marcos, J., Andrés, N., Vázquez, L., 2007. Last glacial maximum and

- deglaciation in central Spanish mountains. *Geophys. Res. Abstr.* 9, 05634. SRef-ID: 1607-7962/gra/EGU2007-A-05634.
- Palacios, D., Marcos, J., Vázquez-Selem, L., 2011. Last glacial maximum and deglaciation of Sierra de Gredos. Central iberian peninsula. *Quat. Int.* 233, 16–26. <https://doi.org/10.1016/j.quaint.2010.04.029>.
- Palacios, D., Andrés, N., Marcos, J., Vázquez-Selem, L., 2012a. Maximum glacial advance and deglaciation of the Pinar Valley (Sierra de Gredos, Central Spain) and its significance in the Mediterranean context. *Geomorphology* 177–178, 51–61. <https://doi.org/10.1016/j.geomorph.2012.07.013>.
- Palacios, D., Andrés, N., Úbeda, J., Alcalá, J., Marcos, J., Vázquez-Selem, L., 2012b. The importance of polygenic moraines in the paleoclimatic interpretation from cosmogenic dating. *Geophys. Res. Abstr.* 14, EGU2012-3759-1.
- Palacios, D., Andrés, N., Marcos, J., Vázquez-Selem, L., 2012c. Glacial landforms and their paleoclimatic significance in Sierra de Guadarrama, central iberian peninsula. *Geomorphology* 139–140, 67–78. <https://doi.org/10.1016/j.geomorph.2011.10.003>.
- Palacios, D., Andrés, N., López-Moreno, J.I., García-Ruiz, J.M., 2015. Late pleistocene deglaciation in the upper gallego valley, central Pyrenees. *Quat. Res.* 83, 397–414. <https://doi.org/10.1016/j.yqres.2015.01.010>.
- Palacios, D., García-Ruiz, J.M., Andrés, N., Schimmelpfennig, I., Campos, N., Leanni, L., ASTER Team, 2017. Deglaciation in the central Pyrenees during the Pleistocene-Holocene transition: timing and geomorphological significance. *Quat. Sci. Rev.* 162, 111–127. <https://doi.org/10.1016/j.quascirev.2017.03.007>.
- Palacios, D., Hughes, P.D., García-Ruiz, J.M., Andrés, N., 2022. The Quaternary ice ages. In: Palacios, D., Hughes, P.D., García-Ruiz, J.M., Andrés, N. (Eds.), *European Glacial Landscapes: Last Deglaciation*. Elsevier, pp. 9–18. <https://doi.org/10.1016/B978-0-12-823498-3.00006-6>.
- Palacios, D., Hughes, P.D., Sánchez-Goni, M.F., García-Ruiz, J.M., Andrés, N., 2023. The terminations of the glacial cycles. In: Palacios, D., Hughes, P.D., García-Ruiz, J.M., Andrés, N. (Eds.), *European Glacial Landscapes: Last Deglaciation*. Elsevier, pp. 11–24. <https://doi.org/10.1016/B978-0-323-91899-2.00002-4>.
- Pallàs, R., Rodés, A., Braucher, R., Carcaillet, J., Ortuño, M., Bordonau, J., Bourlès, D., Vilaplana, J.M., Masana, E., Santanach, P., 2006. Late Pleistocene and Holocene deglaciation in the Pyrenees: a critical review and new evidence from 10Be exposure ages, south-central Pyrenees. *Quat. Sci. Rev.* 25, 2937–2963. <https://doi.org/10.1016/j.quascirev.2006.04.004>.
- Pallàs, R., Rodés, A., Braucher, R., Bourlès, D., Delmas, M., Calvet, M., Gunnell, Y., 2010. Small, isolated glacial catchments as priority targets for cosmogenic surface exposure dating of Pleistocene climate fluctuations, southeastern Pyrenees. *Geology* 38 (10), 891–894. <https://doi.org/10.1130/G31164.1>.
- Pánek, T., Engel, Z., Mentlik, P., Braucher, R., Brežný, M., Skarpich, V., Zondervane, A., 2016. Cosmogenic age constraints on post-LGM catastrophic rock slope failures in the Tatra Mountains (Western Carpathians). *Catena* 138, 52–67. <https://doi.org/10.1016/j.catena.2015.11.005>.
- Pánek, T., Brežný, M., Smedley, R., Winocur, D., Schöenfeld, E., Agliardi, F., Fenn, K., 2023. The largest rock avalanches in Patagonia: timing and relation to Patagonian Ice Sheet retreat. *Quat. Sci. Rev.* 302, 107962. <https://doi.org/10.1016/j.quascirev.2023.107962>.
- Patton, H., Hubbard, A., Bradwell, T., Glasser, N.F., Hambrey, M.J., Clark, C.D., 2013. Rapid marine deglaciation: asynchronous retreat dynamics between the Irish Sea Ice Stream and terrestrial outlet glaciers. *Earth Surf. Dyn.* 1, 277–309. <https://doi.org/10.5194/esurf-d-1-277-2013>.
- Pedraza, J., Fernández, P., 1981. Cuaternario y terciario. In: Ruiz, P., Gabaldón, V. (Eds.), *Mapa Geológico de Bohoyo*. Mapa 577. Instituto Geológico y Minero de España (IGME), Madrid, Spain. <http://www.igme.es/>.
- Pedraza, J., Carrasco, R.M., 2006. El glaciario pleistoceno del Sistema Central. *Enseñanza de las Ciencias de la Tierra* 13 (3), 278–288.
- Pedraza, J., Carrasco, R.M., Domínguez-Villar, D., Villa, J., 2011. Late pleistocene glacial evolutionary stages in the Spanish central system. XVIII INQUA congress, 21st–27th July 2011, Bern, Switzerland, posters. Abstract in. *Quat. Int.* 279–280 (2012), 371–372. <https://doi.org/10.1016/j.quaint.2012.08.1142>.
- Pedraza, J., Carrasco, R.M., Domínguez-Villar, D., Villa, J., 2013. Late pleistocene glacial evolutionary stages in the Gredos mountains (iberian central system). *Quat. Int.* 302, 88–100. <https://doi.org/10.1016/j.quaint.2012.10.038>.
- Pedraza, J., Carrasco, R.M., Villa, J., Soteres, R.L., Karampaglidis, T., Fernández-Lozano, J., 2019. Cirques in the Sierra de Guadarrama and Somosierra mountains (iberian central system): shape, size and controlling factors. *Geomorphology* 341, 153–168. <https://doi.org/10.1016/j.geomorph.2019.05.024>.
- Peltier, C., Kaplan, M.R., Birkel, S.D., Soteres, R.L., Sagredo, E.A., Aravena, J.C., Araos, J., Moreno, P.I., Schwartz, R., Schaefer, J.M., 2021. The large MIS 4 and long MIS 2 glacier maxima on the southern tip of South America. *Quat. Sci. Rev.* 262, 106858. <https://doi.org/10.1016/j.quascirev.2021.106858>.
- Penck, A., 1894. Studien über das Klima Spaniens während der jüngeren Tertiärperiode und der Diluvialperiode. *Z. Ges. Erdkd. Berl.* 29, 109–141. [https://www.digizeitschriften.de/dms/img/?PID=PPN391365657\\_1894\\_0029%7CLOG\\_0017](https://www.digizeitschriften.de/dms/img/?PID=PPN391365657_1894_0029%7CLOG_0017).
- Pérez-Alberti, A., Valcarcel, M., 2022. The glaciers in eastern galicia. In: Oliva, M., Palacios, D., Fernández-Fernández, J.M. (Eds.), *Iberia, Land of Glaciers*. Elsevier, Amsterdam, Netherlands, pp. 375–395. <https://doi.org/10.1016/B978-0-12-821941-6.00018-9> (Chapter 4).14.
- Pérez-González, A., Rubio-Jara, S., Panera, J., Uribelarra, D., 2008. Geocronología de la sucesión arqueostratigráfica de Los Estragales en la Terraza Compleja de Butarque (Valle del río Manzanares, Madrid). *Geogaceta* 45, 39–42. [https://sge.usal.es/publicaciones/geogaceta/2008\\_45.html](https://sge.usal.es/publicaciones/geogaceta/2008_45.html).
- Pratt-Sitaula, B., Burbank, D.W., Heimsath, A.M., Humphrey, N.F., Oskin, M., Putkonen, J., 2011. Topographic control of asynchronous glacial advances: a case study from Annapurna, Nepal. *Geophys. Res. Lett.* 38 (24), L24502. <https://doi.org/10.1029/2011GL049940>.
- Purves, R.S., Mackaness, W.A., Sugden, D.E., 1999. An approach to modelling the impact of snow drift on glaciation in the Cairngorm Mountains, Scotland. *J. Quat. Sci.* 14 (4), 313–321. [https://doi.org/10.1002/\(SICI\)1099-1417\(199907\)14:4<313::AID-JQS457>3.0.CO;2-M](https://doi.org/10.1002/(SICI)1099-1417(199907)14:4<313::AID-JQS457>3.0.CO;2-M).
- Putkonen, J., Swanson, T., 2003. Accuracy of cosmogenic ages for moraines. *Quat. Res.* 59, 255–261. [https://doi.org/10.1016/S0033-5894\(03\)00006-1](https://doi.org/10.1016/S0033-5894(03)00006-1).
- Radbourne, B., 2015. A palaeoclimatic reconstruction of the Cadair Idris area of Snowdonia, using geomorphological evidence from Younger Dryas cirque glaciers. *The Plymouth Student Scientist* 8 (2), 217–257. <http://hdl.handle.net/10026.1/14105>.
- Rasmussen, S.O., Bigler, M., Blockley, S.P., Blunier, T., Buchardt, S.L., Clausen, H.B., et al., 2014. A stratigraphic framework for abrupt climatic changes during the Last Glacial period based on three synchronized Greenland ice-core records: refining and extending the INTIMATE event stratigraphy. *Quat. Sci. Rev.* 106, 14–28. <https://doi.org/10.1016/j.quascirev.2014.09.007>.
- Reade, H., Tripp, J.A., Charlton, S., Grimm, S., Sayle, K.L., Fensome, A., Higham, T.F.G., Barnes, I., Stevens, R.E., 2020. Radiocarbon chronology and environmental context of Last Glacial Maximum human occupation in Switzerland. *Sci. Rep.* 10, 4694. <https://doi.org/10.1038/s41598-020-61448-7>.
- Reber, R., Akçar, N., Tikhomirov, D., Yesilyurt, S., Vockenhuber, C., Yavuz, V., Ivy-Ochs, S., Schlüchter, C., 2022. LGM glaciations in the northeastern anatolian mountains: new insights. *Geosciences* 12 (7), 257. <https://doi.org/10.3390/geosciences12070257>.
- Ribolini, A., Spagnolo, M., Giraudi, C., 2022a. The Italian mountains: glacial landforms from the Last Glacial Maximum. In: Palacios, D., Hughes, P.D., García-Ruiz, J.M., Andrés, N. (Eds.), *European Glacial Landscapes: Maximum Extent of Glaciations*. Elsevier, pp. 481–486. <https://doi.org/10.1016/B978-0-12-823498-3.00022-4>.
- Ribolini, A., Spagnolo, M., Cyr, A.J., Federici, P.R., 2022b. Last glacial maximum and early deglaciation in the stura valley, southwestern European Alps. *Quat. Sci. Rev.* 295, 107770. <https://doi.org/10.1016/j.quascirev.2022.107770>.
- Ribolini, A., Spagnolo, M., Giraudi, C., 2023. The Italian Mountains: glacial landforms during deglaciation. In: Palacios, D., Hughes, P.D., García-Ruiz, J.M., Andrés, N. (Eds.), *European Glacial Landscapes: Last Deglaciation*. Elsevier, pp. 209–220. <https://doi.org/10.1016/B978-0-323-91899-2.00041-3>.
- Rodríguez-Rodríguez, L., Jiménez-Sánchez, M., Domínguez-Cuesta, M.J., Rinterknecht, V., Pallàs, R., Bourlès, D., Valero-Garcés, B., 2014. A multiple dating-method approach applied to the Sanabria Lake moraine complex (NW Iberian Peninsula, SW Europe). *Quat. Sci. Rev.* 83, 1–10. <https://doi.org/10.1016/j.quascirev.2013.10.019>.
- Rodríguez-Rodríguez, L., Jiménez-Sánchez, M., Domínguez-Cuesta, M.J., Aranburu, A., 2015. Research history on glacial geomorphology and geochronology of the Cantabrian Mountains, north Iberia (43–42°N/7–2°W). *Quat. Int.* 364, 6–21. <https://doi.org/10.1016/j.quaint.2014.06.007>.
- Rodríguez-Rodríguez, L., Jiménez-Sánchez, M., Domínguez-Cuesta, M.J., Rinterknecht, V., Pallàs, R., Bourlès, D., 2016. Chronology of glaciations in the cantabrian mountains (NW Iberia) during the last glacial cycle based on in situ-produced <sup>10</sup>Be. *Quat. Sci. Rev.* 138, 31–48. <https://doi.org/10.1016/j.quascirev.2016.02.027>.
- Rodríguez-Rodríguez, L., Jiménez-Sánchez, M., Domínguez-Cuesta, M.J., Rinterknecht, V., Pallàs, R., Aumaître, G., Bourlès, D.L., Keddadouche, K., 2017. Timing of last deglaciation in the Cantabria mountains (Iberian Peninsula; North Atlantic region) based on in situ-produced 10Be exposure dating. *Quat. Sci. Rev.* 171, 166–181. <https://doi.org/10.1016/j.quascirev.2017.07.012>.
- Rodríguez-Rodríguez, L., Domínguez-Cuesta, M.J., Rinterknecht, V., Jiménez-Sánchez, M., Saúl González-Lemos, S., Léanni, L., Sanjurjo, J., Ballesteros, D., Valenzuela, P., Llana-Fúnez, S., ASTER Team, 2018. Constraining the age of superimposed glacial records in mountain environments with multiple dating methods (Cantabrian Mountains, Iberian Peninsula). *Quat. Sci. Rev.* 195, 215–231. <https://doi.org/10.1016/j.quascirev.2018.07.025>.
- Rolland, Y., Darnault, R., Braucher, R., Bourlès, D., Petit, C., Bouissou, S., ASTER Team, 2020. Deglaciation history at the Alpine-Mediterranean transition (Argentiera-Mercantour, SW Alps) from 10Be dating of moraines and glacially polished bedrock. *Earth Surf. Process. Landforms* 45 (2), 393–410. <https://doi.org/10.1002/esp.4740>.
- Rubiales, J.M., García-Amorena, I., Hernández, L., Génova, M., Martínez, F., Gómez-Manzanque, F., Morla, C., 2010. Late quaternary dynamics of pinewoods in the iberian mountains. *Rev. Palaeobot. Palynol.* 162, 476–491. <https://doi.org/10.1016/j.revpalbo.2009.11.008>.
- Rubio, J.C., Pedraza, J., Carrasco, R.M., 1992. Reconocimiento de tills primarios en el sector central de la Sierra de Gredos (Sistema Central Español). In: López Bermúdez, F., Conesa García, C., Romero Díaz, M.A. (Eds.), *Estudios de Geomorfología en España I*. SEG, Murcia, pp. 413–422.
- Ruiz-Fernández, J., Oliva, M., Cruces, A., Lopes, V., Freitas, M.C., Andrade, C., García-Hernández, C., López-Sáez, J.A., Geraldés, M., 2016. Environmental evolution in the Picos de Europa (cantabrian mountains, SW Europe) since the last glaciation. *Quat. Sci. Rev.* 138, 87–104. <https://doi.org/10.1016/j.quascirev.2016.03.002>.
- Ruiz-Fernández, J., García-Hernández, C., Gallinar-Cañedo, D., 2022. The glaciers of the Picos de Europa. In: Oliva, M., Palacios, D., Fernández-Fernández, J.M. (Eds.), *Iberia, Land of Glaciers*. Elsevier, Amsterdam, Netherlands. <https://doi.org/10.1016/B978-0-12-821941-6.00012-8> (Chapter 4), 8, 237–263.
- Ruszkiczay-Rüdiger, Z., Kern, Z., Urdea, P., Madarász, B., Braucher, R., ASTER Team,

2021. Limited glacial erosion during the last glaciation in mid-latitude cirques (Retezat Mts. Southern Carpathians, Romania). *Geomorphology* 384, 107719. <https://doi.org/10.1016/j.geomorph.2021.107719>.
- Salvador-Franch, F., Andrés, N., Gómez-Ortiz, A., Palacios, D., 2022. The glaciers of the southeastern Pyrenees. In: Oliva, M., Palacios, D., Fernández-Fernández, J.M. (Eds.), *Iberia, Land of Glaciers*. Elsevier, Amsterdam, Netherlands. <https://doi.org/10.1016/B978-0-12-821941-6.00028-1> (Chapter 4), 61–85.
- Sánchez-Goni, M.F., Landais, A., Fletcher, W.J., Naughton, F., Desprat, S., Duprat, J., 2008. Contrasting impacts of Dansgaard–Oeschger events over a western European latitudinal transect modulated by orbital parameters. *Quat. Sci. Rev.* 27 (11–12), 1136–1151. <https://doi.org/10.1016/j.quascirev.2008.03.003>.
- Sánchez-López, G., Hernández, A., Pla-Rabes, S., Trigo, R.M., Toro, M., Granados, I., Sáez, A., Masqué, P., Pueyo, J.J., Rubio-Ingles, M.J., Giral, S., 2016. Climate reconstruction for the last two millennia in central Iberia: the role of east atlantic (EA), North Atlantic oscillation (NAO) and their interplay over the iberian peninsula. *Quat. Sci. Rev.* 149, 135–150. <https://doi.org/10.1016/j.quascirev.2016.07.021>.
- Santisteban, J.L., Schulte, L., 2007. Fluvial networks of the Iberian Peninsula: a chronological framework. *Quat. Sci. Rev.* 26, 2738–2757. <https://doi.org/10.1016/j.quascirev.2006.12.019>.
- Santos-González, J., Redondo-Vega, J.M., García-de-Celis, A., González-Gutiérrez, R.B., Gómez-Villar, A., 2022. The glaciers of the Leonese cantabrian mountains. In: Oliva, M., Palacios, D., Fernández-Fernández, J.M. (Eds.), *Iberia, Land of Glaciers*. Elsevier, Amsterdam, Netherlands. <https://doi.org/10.1016/B978-0-12-821941-6.00014-1> (Chapter 4), 10, 289–314.
- Sanz-Donaire, J.J., 1979. *El corredor de Béjar*. Tomo I. Instituto de Geografía Aplicada, CSIC, Madrid, p. 195.
- Sarikaya, M.A., Çiner, A., 2017. Late quaternary glaciations in the eastern mediterranean. *Geol. Soc. London, Spec. Pub.* 433, 289–305. <https://doi.org/10.1144/SP433.4>.
- Sarikaya, M.A., Zreda, M., Ciner, A., Zweck, C., 2008. Cold and wet Last Glacial Maximum on Mount Sandıras, SW Turkey, inferred from cosmogenic dating and glacier modelling. *Quat. Sci. Rev.* 27, 769–780. <https://doi.org/10.1016/j.quascirev.2008.01.002>.
- Scapozza, C., Castelletti, C., Soma, L., Dall'Agnolo, S., Ambrosi, C., 2014. Timing of LGM and deglaciation in the southern Swiss Alps. *Quater. Geomorphol.* 20 (4), 307–322. <https://doi.org/10.4000/geomorphologie.10753>.
- Seret, G., Dricot, J., Wansard, G., 1990. Evidence for an early glacial maximum in the French Vosges during the last glacial cycle. *Nature* 346, 453–456. <https://doi.org/10.1038/346453a0>.
- Serra, E., Valla, P.G., Gribenski, N., Carcaillet, J., Deline, P., 2022. Post-LGM glacial and geomorphic evolution of the Dora Baltea valley (western Italian Alps). *Quat. Sci. Rev.* 282, 107446. <https://doi.org/10.1016/j.quascirev.2022.107446>.
- Serrano, E., González Trueba, J.J., González García, M., 2012. Mountain glaciation and paleoclimatic reconstruction in the Picos de Europa (iberian peninsula, SW Europe). *Quat. Res.* 78, 303–314. <https://doi.org/10.1016/j.yqres.2012.05.016>.
- Serrano, E., González-Trueba, J.J., Pellitero, R., González-García, M., Gómez-Lende, M., 2013a. Quaternary glacial evolution in the central Cantabrian mountains (Northern Spain). *Geomorphology* 196, 65–82. <https://doi.org/10.1016/j.geomorph.2012.05.001>.
- Serrano, E., Gómez-Lende, M., González Trueba, J.J., Turu, V., Ros, X., 2013b. Fluctuaciones glaciares pleistocenas y cronología en las Montañas Pasiegas (Cordillera Cantábrica). *Revista Cuaternario y Geomorfología* 27 (1–2), 91–110.
- Serrano, E., Gómez-Lende, M., Pellitero, R., González Trueba, J.J., 2015. Deglaciation in the cantabrian mountains: pattern and evolution. *Cuadernos de Investigación Geográfica* 41 (2), 389–408. <https://doi.org/10.18172/cig.2716>.
- Serrano, E., Gómez-Lende, M., Pisabarro, A., 2022. The glaciers of the western massifs of Cantabria. In: Oliva, M., Palacios, D., Fernández-Fernández, J.M. (Eds.), *Iberia, Land of Glaciers*. Elsevier, Amsterdam, Netherlands. <https://doi.org/10.1016/B978-0-12-821941-6.00010-4> (Chapter 4), 6, 201–219.
- Shakun, J.D., Carlson, A.M., 2010. A global perspective on Last Glacial Maximum to Holocene climate change. *Quat. Sci. Rev.* 29, 1801–1816. <https://doi.org/10.1016/j.quascirev.2010.03.016>.
- Shakun, J.D., Clark, P.U., He, F., Marcott, S.A., Mix, A.C., Liu, Z., Otto-Bliesner, B., Schmittner, A., Bard, E., 2012. Global warming preceded by increasing carbon dioxide concentrations during the last deglaciation. *Nature* 484 (7392), 49–54. <https://doi.org/10.1038/nature10915>.
- Shakun, J.D., Clark, P.U., He, F., Lifton, N.A., Liu, Z., Otto-Bliesner, B.L., 2015. Regional and global forcing of glacier retreat during the last deglaciation. *Nat. Commun.* 6, 8059. <https://doi.org/10.1038/ncomms9059>.
- Silva, P.G., López-Recio, M., Cuartero, F., Baena, J., Tapias, F., Manzano, I., Martín, D., Morín, J., Roquero, E., 2012. Contexto geomorfológico y principales rasgos tecnológicos de nuevos yacimientos del Pleistoceno Medio y Superior en el Valle Inferior del Manzanares (Madrid, España). *Estud. Geol.* 68 (1), 57–89. <https://doi.org/10.3989/egol.40338.134>.
- Silva, P.G., Roquero, E., López-Recio, M., Huerta, P., Martínez-Graña, A.M., 2017. Chronology of fluvial terrace sequences for large Atlantic rivers in the Iberian Peninsula (Upper Tagus and Duero drainage basins, Central Spain). *Quat. Sci. Rev.* 166, 188–203. <https://doi.org/10.1016/j.quascirev.2016.05.027>.
- Sinnl, G., Adolphi, F., Christl, M., Welten, K.C., Woodruff, T., Caffee, M., Svensson, A., Muscheler, R., Rasmussen, S.O., 2022. *Clim. Past Discuss.*, Preprint under Review for CP. In: Synchronizing Ice-Core and U/Th Time Scales in the Last Glacial Maximum Using Hulu Cave 14C and New 10Be Measurements from Greenland and Antarctica. <https://doi.org/10.5194/cp-2022-62>.
- Smith, M.J., Rose, J., Booth, S., 2006. Geomorphological mapping of glacial landforms from remotely sensed data: an evaluation of the principal data sources and an assessment of their quality. *Geomorphology* 76 (1–2), 148–165. <https://doi.org/10.1016/j.geomorph.2005.11.001>.
- Soteres, R.L., Pedraza, J., Carrasco, R.M., 2020. Snow avalanche susceptibility of the circo de Gredos (iberian central system, Spain). *J. Maps* 16 (2), 155–165. <https://doi.org/10.1080/17445647.2020.1717655>.
- Spagnolo, M., Rea, B.R., Barr, I., 2022. The (mis)conception of average Quaternary conditions. *Quat. Res.* 105, 235–240. <https://doi.org/10.1017/qua.2021.48>.
- Spötl, C., Koltai, G., Jarosch, A.H., Cheng, H., 2021. Increased autumn and winter precipitation during the last glacial maximum in the European Alps. *Nat. Commun.* 12, 1839. <https://doi.org/10.1038/s41467-021-22090-7>.
- Staiger, J.K.W., Gosse, J.C., Johnson, J.V., Fastook, J., Gray, J.T., Stockli, D.F., Stockli, L., Finkel, R., 2005. Quaternary relief generation by polythermal glacier ice. *Earth Surf. Process. Landforms* 30, 1145–1159. <https://doi.org/10.1002/esp.1267>.
- Starr, A., Hall, I.R., Barker, S., Rackow, T., Zhang, X., Hemming, S.R., et al., 2021. Antarctic icebergs reorganize ocean circulation during Pleistocene glacials. *Nature* 589 (7841), 236–241. <https://doi.org/10.1038/s41586-020-03094-7>.
- Stroeven, A.P., Fabel, D., Harbor, J.M., Fink, D., Caffee, M.W., Dahlgren, T., 2011. Importance of sampling across an assemblage of glacial landforms for interpreting cosmogenic ages of deglaciation. *Quat. Res.* 76 (1), 148–156. <https://doi.org/10.1016/j.yqres.2011.04.004>.
- Svensson, A., Dahl-Jensen, D., Steffensen, J.P., Blunier, T., Rasmussen, S.O., Vinther, B.M., Bigler, M., 2020. Bipolar volcanic synchronization of abrupt climate change in Greenland and Antarctic ice cores during the last glacial period. *Clim. Past* 16 (4), 1565–1580. <https://doi.org/10.5194/cp-16-1565-2020>.
- Thackray, G.D., Owen, L.A., Yi, C., 2008. Timing and nature of late Quaternary Mountain glaciation. *J. Quat. Sci.* 23 (6–7), 503–508. <https://doi.org/10.1002/jqs.1225>.
- Tomkins, M.D., Dortch, J.M., Hughes, P.D., Huck, J.J., Pallás, R., Rodés, A., Allard, J.L., Stimson, A.G., Bourlès, D., Rinterknecht, V., Jomelli, V., Rodríguez-Rodríguez, L., Copons, R., Barr, I.D., Darvill, C.M., Bishop, T., 2021. Moraine crest or slope: an analysis of the effects of boulder position on cosmogenic exposure age. *Earth Planet Sci. Lett.* 570. <https://doi.org/10.1016/j.epsl.2021.117092>.
- Toucanne, S., Soulet, G., Freslon, N., Jacinto, R.S., Dennielou, B., Zaragosi, S., et al., 2015. Millennial-scale fluctuations of the European Ice Sheet at the end of the last glacial, and their potential impact on global climate. *Quat. Sci. Rev.* 123, 113–133. <https://doi.org/10.1016/j.quascirev.2015.06.010>.
- Toucanne, S., Landais, A., Naughton, F., Rodrigues, T., Vázquez Riveiros, N., Sánchez-Goni, M.F., 2022. The global last glacial maximum: the eastern North Atlantic (marine sediments) and the Greenland ice sheet climatic signal. In: Palacios, D., Hughes, P.D., García-Ruiz, J.M., Andrés, N. (Eds.), *European Glacial Landscapes: Maximum Extent of Glaciations*. Elsevier, pp. 89–194. <https://doi.org/10.1016/B978-0-12-823498-3.00052-2>.
- Turu, V., 2023. *Asymmetries within the Pyrenees and Correlation across the Westernmost European Mountain Ranges. In: Mid-Late Pleistocene Glacial Dynamics in the Valira Valleys (Principality of Andorra)*. Barcelona Univ, Barcelona, Spain. Ph.D. Thesis.
- Turu, V., Carrasco, R.M., Pedraza, J., Ros, X., Ruiz-Zapata, B., Soriano-López, J.M., Mur-Cacahu, E., Pélachs-Mañosa, A., Muñoz-Martín, A., Sánchez, J., Echeverría-Moreno, A., 2018. Late glacial and post-glacial deposits of the Navamúno peatbog (Iberian Central System): chronology and paleoenvironmental implications. *Quat. Int.* 470, 82–95. <https://doi.org/10.1016/j.quaint.2017.08.018>.
- Turu, V., Carrasco, R.M., López-Sáez, J.A., Pontevedra-Ponval, J., Pedraza, J., Luemo-Lautenschlaeger, R., et al., 2021. Paleoenvironmental changes in the Iberian central system during the Late-glacial and Holocene as inferred from geochemical data: a case study of the Navamúno depression in western Spain. *Catena* 207, 105689. <https://doi.org/10.1016/j.catena.2021.105689>.
- Uppala, S.M., Kallberg, P.W., Simmons, A.J., et al., 2005. The ERA-40 re-analysis. *Q. J. R. Meteorol. Soc.* 131, 2961–3012. <https://doi.org/10.1256/qj.04.176>.
- van der Knaap, W.O., van Leeuwen, J.F.N., 1997. Late Glacial and Early Holocene vegetation succession altitudinal vegetation zonation, and climatic change in the Serra da Estrela. *Port. Rev. Palaeobot. Palynol.* 97, 239–285. [https://doi.org/10.1016/S0034-6667\(97\)00008-0](https://doi.org/10.1016/S0034-6667(97)00008-0).
- van Raden, U.J., Colombaroli, D., Gilli, A., Schwander, J., Bernasconi, S.M., van Leeuwen, J., Leuenberger, M., Eicher, U., 2013. High-resolution late-glacial chronology for the Gerzensee lake record (Switzerland): d18O correlation between a Gerzensee-stack and NGRIP. *Palaeogeogr. Palaeoclimatol. Palaeoecol.* 391, 13–24. <https://doi.org/10.1016/j.palaeo.2012.05.017>.
- Vasskog, K., Langebroek, P.M., Andrews, J.T., Nilsen, J.E.Ø., Nesje, A., 2015. The Greenland Ice Sheet during the last glacial cycle: current ice loss and contribution to sea-level rise from a palaeoclimatic perspective. *Earth Sci. Rev.* 150, 45–67. <https://doi.org/10.1016/j.earscirev.2015.07.006>.
- Vaudour, J., 1979. *La Région de Madrid. Altérations, sols et paléosols*. In: *Contribution à l'étude géomorphologique d'une région méditerranéenne semi-aride*, vol. 390. Ophrys, Paris.
- Ventura, J., Turu, V., 2022. The glaciers of the central-eastern Pyrenees. In: Oliva, M., Palacios, D., Fernández-Fernández, J.M. (Eds.), *Iberia, Land of Glaciers*. Elsevier, Amsterdam, Netherlands. <https://doi.org/10.1016/B978-0-12-821941-6.00006-2> (Chapter 4), 2, 87–121.
- Vidal-Box, C., 1948. Nuevas aportaciones al conocimiento geomorfológico de la Cordillera Central. *Estud. Geográficos* 9 (30), 5–52.
- Vieira, G., 2008. Combined numerical and geomorphological reconstruction of the Serra da Estrela plateau icefield. *Portugal. Geomorphology*. 97, 190–207. <https://doi.org/10.1016/j.geomorph.2007.02.042>.
- Vieira, G., Ferreira, A.B., Mycielska-Dowgiallo, E., Woronko, B., Olszak, I., 2001.

- Thermoluminescence Dating of Fluvio-glacial Sediments (Serra da Estrela, Portugal). *V REQUI/I CQPLI, Lisboa, Portugal*, pp. 85–92.
- Vieira, G., Palacios, D., Andrés, N., Mora, C., Vázquez-Salem, L., Woronko, B., Soncco, C., Úbeda, J., Goyanes, G., 2021. Penultimate Glacial Cycle glacier extent in the Iberian Peninsula: new evidence from the Serra da Estrela (Central System, Portugal). *Geomorphology* 388, 107781. <https://doi.org/10.1016/j.geomorph.2021.107781>.
- Vieira, G., Woronko, B., 2022. The glaciers of Serra da Estrela. In: Oliva, M., Palacios, D., Fernández-Fernández, J.M. (Eds.), *Iberia, Land of Glaciers*. Elsevier, Amsterdam, Netherlands, pp. 417–435. <https://doi.org/10.1016/B978-0-12-821941-6.00020-7> (Chapter 4), 16.
- Voelker, A.H.L., de Abreu, L., Schönfeld, J., Erlenkeuser, H., Abrantes, F., 2009. Hydrographic conditions along the western Iberian margin during marine isotope stage 2. *G-cubed* 10 (12), Q12U08. <https://doi.org/10.1029/2009GC002605>.
- Weixelman, D.A., Hill, B., Cooper, D.J., Berlow, E.L., Viers, J.H., Purdy, S.E., Merrill, A.G., Gross, S.E., 2011. A Field Key to Meadow Hydrogeomorphic Types for the Sierra Nevada and Southern Cascade Ranges in California. *Gen. Tech. Rep. R5-TP-034*. U.S. Department of Agriculture, Forest Service, Pacific Southwest Region, Vallejo, CA, p. 34. [https://www.fs.usda.gov/Internet/FSE\\_DOCUMENTS/stelprdb5362593.pdf](https://www.fs.usda.gov/Internet/FSE_DOCUMENTS/stelprdb5362593.pdf).
- Wirsig, Ch, Zasadni, J., Christl, M., Akçar, N., Ivy-Ochs, S., 2016. Dating the onset of LGM ice surface lowering in the High Alps. *Quat. Sci. Rev.* 143, 37–50. <https://doi.org/10.1016/j.quascirev.2016.05.001>.
- Wolf, D., Kolb, T., Ryborz, K., Heinrich, S., Schäfer, I., Calvo, R., Sánchez, J., Hambach, U., Zech, R., Zöller, L., Faust, D., 2021. Evidence for strong relations between the upper Tagus loess formation (central Iberia) and the marine atmosphere off the Iberian margin during the last glacial period. *Quat. Res.* 101, 84–113. <https://doi.org/10.1017/qua.2020.119>.
- Wygall, B.T., Heidenreich, S.M., 2014. Deglaciation and human colonization of northern Europe. *J. World PreHistory* 27, 111–144. <https://doi.org/10.1007/s10963-014-9075-z>.
- Yalcin, M., 2019. The impact of topographical parameters to the glaciation and glacial retreat on Mount Ağrı (Ararat). *Environ. Earth Sci.* 78, 393. <https://doi.org/10.1007/s12665-019-8374-1>.
- Zasadni, J., Klapyska, P., Makos, M., 2022. The tatra mountains: glacial landforms from the last glacial maximum. In: Palacios, D., Hughes, P.D., García-Ruiz, J.M., Andrés, N. (Eds.), *European Glacial Landscapes: Maximum Extent of Glaciations*. Elsevier, pp. 435–440. <https://doi.org/10.1016/B978-0-12-823498-3.00049-2>.